JCI The Journal of Clinical Investigation

The long non-coding RNA CARDINAL attenuates cardiac hypertrophy by modulating protein translation

Xin He, … , Da-Zhi Wang, Zhan-Peng Huang

J Clin Invest. 2024. https://doi.org/10.1172/JCI169112.

Research In-Press Preview Cardiology Development

One of the features of pathological cardiac hypertrophy is enhanced translation and protein synthesis. Translational inhibition has been shown to be an effective means of treating cardiac hypertrophy, although system-wide side effects are common. Regulators of translation, such as cardiac-specific long non-coding RNAs (lncRNAs), could provide new, more targeted, therapeutic approaches to inhibit cardiac hypertrophy. Therefore, we generated mice lacking a previously identified lncRNA named *CARDINAL* to examine its cardiac function. We demonstrate that *CARDINAL* is a cardiac-specific, ribosome associated lncRNA and show that its expression is induced in the heart upon pathological cardiac hypertrophy; its deletion in mice exacerbates stress-induced cardiac hypertrophy and augments protein translation. In contrast, overexpression of *CARDINAL* attenuates cardiac hypertrophy in vivo and in vitro, and suppresses hypertrophy-induced protein translation. Mechanistically, *CARDINAL* interacts with developmentally regulated GTP binding protein 1 (DRG1) and blocks its interaction with DRG family regulatory protein 1 (DFRP1); as a result, DRG1 is downregulated, thereby modulating the rate of protein translation in the heart in response to stress. This study provides evidence for the therapeutic potential of targeting cardiac-specific lncRNAs to suppress disease-induced translational changes and to treat cardiac hypertrophy and heart failure.

The long non-coding RNA CARDINAL attenuates cardiac hypertrophy by modulating protein translation

Xin He[1,2,3*], Tiqun Yang[1,3*], Yao Wei Lu[2,4,8*], Gengze Wu[2], Gang Dai[3], Qing Ma[2], Mingming Zhang[2], Huimin Zhou[1,3], Tianxin Long[1,3], Youchen Yan[1,3], Zhuomin Liang[1,2,3], Chen Liu[1,3], William T. Pu[2], Yugang Dong[1,3], Jingsong Ou[3,5], Hong Chen[4], John D. Mably[6], Jiangui He[1,3#], Da-Zhi Wang[2,6,7#], Zhan-Peng Huang[1,3,5#]

[1]Department of Cardiology, Center for Translational Medicine, Institute of Precision Medicine, The First Affiliated Hospital, Sun Yat-sen University, Guangzhou 510080, China

[2]Department of Cardiology, Boston Children's Hospital, Harvard Medical School, 320 Longwood Avenue, Boston, MA 02115, USA

[3]NHC Key Laboratory of Assisted Circulation, Sun Yat-sen University, Guangzhou, China

[4]Vascular Biology Program, Department of Surgery, Boston Children's Hospital, Harvard Medical School, 320 Longwood Avenue, Boston, MA 02115, USA

[5]National-Guangdong Joint Engineering Laboratory for Diagnosis and Treatment of Vascular Diseases, Guangzhou 510080, China

[6]Center for Regenerative Medicine, USF Health Heart Institute, Morsani College of Medicine, University of South Florida, Tampa, FL 33602, USA

[7]Departments of Internal Medicine, Molecular Pharmacology & Physiology, Morsani College of Medicine, University of South Florida, Tampa, FL 33602, USA

[8]Present address for Dr. Lu: Department of Medicine and Hastings Center for Pulmonary Research, Keck School of Medicine, University of Southern California, Los Angeles, CA 90033, USA

[#]Corresponding authors:

Zhan-Peng Huang; huangzhp27@mail.sysu.edu.cn, +86-20 8761 8634 (tel)
Department of Cardiology, Center for Translational Medicine, Institute of Precision Medicine, The First Affiliated Hospital, Sun Yat-sen University, Guangzhou 510080, China

Jiangui He, hejg@mail.sysu.edu.cn, +86-20 8761 8634 (tel)
Department of Cardiology, Center for Translational Medicine, Institute of Precision Medicine, The First Affiliated Hospital, Sun Yat-sen University, Guangzhou 510080, China

Da-Zhi Wang; email: dazhiw@usf.edu, +1-813-396-0078 (tel)
Department of Cardiology, Boston Children's Hospital, Harvard Medical School, 320 Longwood Avenue, Boston, MA 02115, USA

*These three authors share the first author position

Short Title: The lncRNA *CARDINAL* reduces cardiac hypertrophy

Conflict-of-interest statement:
The authors have declared that no conflict of interest exists.

Abstract

One of the features of pathological cardiac hypertrophy is enhanced translation and protein synthesis. Translational inhibition has been shown to be an effective means of treating cardiac hypertrophy, although system-wide side effects are common. Regulators of translation, such as cardiac-specific long non-coding RNAs (lncRNAs), could provide new, more targeted, therapeutic approaches to inhibit cardiac hypertrophy. Therefore, we generated mice lacking a previously identified lncRNA named *CARDINAL* to examine its cardiac function. We demonstrate that *CARDINAL* is a cardiac-specific, ribosome associated lncRNA and show that its expression is induced in the heart upon pathological cardiac hypertrophy; its deletion in mice exacerbates stress-induced cardiac hypertrophy and augments protein translation. In contrast, overexpression of *CARDINAL* attenuates cardiac hypertrophy *in vivo* and *in vitro*, and suppresses hypertrophy-induced protein translation. Mechanistically, *CARDINAL* interacts with developmentally regulated GTP binding protein 1 (DRG1) and blocks its interaction with DRG family regulatory protein 1 (DFRP1); as a result, DRG1 is downregulated, thereby modulating the rate of protein translation in the heart in response to stress. This study provides evidence for the therapeutic potential of targeting cardiac-specific lncRNAs to suppress disease-induced translational changes and to treat cardiac hypertrophy and heart failure.

Key words: Cardiac hypertrophy, lncRNA, Translational regulation, DRG1, Ribosome

Introduction

Heart failure is the common end-stage for most cardiomyopathies; it exhibits both a high prevalence and mortality rate (1, 2). Although past decades have witnessed great progress in short-term heart failure treatment, its long-term prognosis remains poor (2). Pathological cardiac hypertrophy is one of the driving forces in heart failure. Numerous studies have demonstrated that inhibition of cardiac hypertrophy under stress condition contributes to the preservation of cardiac function (3).

Translation is enhanced during the development of cardiac hypertrophy (4); however, we have a limited understanding of the mechanisms regulating translation and few approaches for therapeutic intervention. In fact, most published mechanistic studies of cardiac hypertrophy have focused on transcriptional regulation (5). Unfortunately, these studies have limited value for the development of treatments for hypertrophy since mRNA levels only moderately correlate with protein amounts (6). Our previous studies highlighted the importance of translational regulation in cardiac hypertrophy and the importance of its continued interrogation as a mechanism and potential target for clinical intervention (7, 8).

The imbalance of protein synthesis and degradation is the underlying cause for the increased heart weight reported in cardiac hypertrophy. Studies have confirmed that translational inhibition achieved by modulating regulatory protein activity was efficient in suppressing cardiac hypertrophy, while translation promotion exacerbated cardiac hypertrophy (9-11). However, most of these regulatory proteins were constitutively expressed, with functions in multiple tissues; the targeting of these molecules inevitably led to system-wide side effects. For example, Mammalian target of rapamycin (mTOR) is an important protein

kinase that regulates the rate of translation (12). Preclinical and clinical data showed that mTOR inhibitors were effective in reversing cardiac hypertrophy (13-16). However, these therapies have potential to cause serious side effects, such as immunosuppression and thrombocytopenia, which is not an acceptable risk in treatments for heart failure (17). In principle, the characterization of cardiac-specific translational regulators would identify safer and new therapeutic targets for cardiac hypertrophy and heart failure. The underlying concepts that prompted our investigation of lncRNA molecules as potential cardiac-specific translational regulators included published reports demonstrating that; 1) lncRNAs typically demonstrate a higher tissue specificity compared with protein coding genes (18); and 2) many lncRNAs without coding potential have been found to be associated with the ribosome, which indicates a potential role in regulating ribosomal function (19-21).

In this study, we investigate the function of a cardiac-specific, translation altering lncRNA, which was previously identified as a serum response factor interacting lncRNA and named Myocardin-adjacent long noncoding RNA, abbreviated *CARDINAL* (22). Here, we report that *CARDINAL* is associated with the ribosome to suppress translation in cardiomyocytes under stress conditions. Loss of *CARDINAL* exacerbates cardiac hypertrophy in response to stress. Mechanistically, we show that *CARDINAL* interacts with developmentally regulated GTP binding protein 1 (DRG1), an enhancer of translation. We also demonstrate that *CARDINAL* promotes the degradation of DRG1 by preventing its interaction with the DRG1 stabilizing partner DFRP1, the DRG family-regulatory protein 1.

Results

Screening and identification of *CARDINAL* as a cardiac-specific ribosome associated lncRNA

The objective of this analysis was the identification of cardiac-specific ribosome associated lncRNAs from the human genome. To identify cardiac-specific lncRNAs, our initial analysis was performed using large RNA sequencing datasets generated from seven major organs, in seven species, across multiple developmental time points (23). Since the onset of cardiac hypertrophy and heart failure is more common in the elderly, we focused on adult human samples; these included 2 heart samples, 9 brain samples, 9 cerebellum samples, 6 liver samples, and 6 testis samples (there were no kidney or ovary samples from human adults). To ensure cardiac specificity, we focused on lncRNAs in hearts with a FPKM value 5 times greater than in any of the other samples; this initial screening yielded 96 candidate lncRNAs (Figure 1A). Among these lncRNAs, we excluded 70 that did not have an Ensembl annotation and 18 that did not have an orthologue in mouse (Figure 1A and 1B). The remaining 8 lncRNAs were cross-checked for cardiac specificity using adult mice tissues to ensure their conservation in expression between human and mouse. Three lncRNAs were further excluded because of the low cardiac specificity of the mouse orthologues (Figure 1A, 1C and Suppl. Figure 1).

We next examined the association of the 5 candidate lncRNAs with the ribosome. Lysates of human embryonic stem cell derived cardiomyocytes (hESC-CMs) were subjected to polysome profiling to separate ribosome-free fractions and polysome fractions. RNA isolated from these fractions were subjected to RNA-seq (24, 25). Four of the 5 candidates could be detected in the polysome fractions; among them, *CARDINAL* (LINC00670) exhibited the

strongest association (Figure 1D); the orthologue of *CARDINAL* in mouse, Gm12295, was found to be associated with the ribosome and detected in the polysome fraction of heart (Figure 1E). Interestingly, polysome-associated *CARDINAL* increased during cardiac hypertrophy induced by transverse aortic constriction (TAC) (Figure 1E). To verify the association of *CARDINAL* with the ribosome, we performed polysome profiling followed by real time quantitative polymerase chain reaction (RT-qPCR); *CARDINAL* could be detected in the 40S, 60S, monosome, and polysome fraction, but not in ribosome-free fraction (Figure 1F). This distribution pattern was distinct from that of the translated transcript for *Gapdh* mRNA, suggesting that the function of *CARDINAL* is linked to its association with the ribosome (Figure 1F). Together, these data demonstrate that *CARDINAL* is a ribosome-associated lncRNA.

CARDINAL was previously described as a cardiac enriched lncRNA that interacts with SRF to regulate cardiac gene expression (22). Cardiac specific expression of *Cardinal* in mouse was validated by RT-qPCR (Suppl. Figure 2). Furthermore, we found that the expression of *Cardinal* in the heart gradually increased from embryonic and postnatal stages to adult, with highest expression detected in 6 month-old mouse hearts (Suppl. Figure 2), supporting a role in adult hearts. We separated cardiomyocyte and non-cardiomyocyte fractions from adult mouse hearts using the Langendorff procedure and found that *Cardinal* was predominantly expressed in cardiomyocytes; as expected, the control markers cardiac troponin T (*cTnT*) and periostin (*Postn*) were expressed in cardiomyocyte and fibroblast fractions, respectively (Figure 1G). We confirmed that the full-length *Cardinal* transcript is approximately 3 kb in length using rapid amplification of cDNA ends (RACEs) and Northern blotting approaches (Figure 1H), as previously reported (22). Ribo-seq data indicated that the first 2 exons were

associated with the ribosome (26), but PhyloCSF scoring did not indicate any coding potential in these regions (Figure 1I); these results suggested that *Cardinal* was a non-coding RNA. This conclusion was supported by a previous large-scale, cardiac translatomic study which did not annotate *CARDINAL* as a translated RNA in either mouse or human (26). Moreover, a previous report also described *CARDINAL* as a non-coding RNA expressed in the heart (22). Both mouse and human *CARDINAL* have 2 highly conserved regions near the transcriptional start site (Figure 1I), indicating that the transcription of *CARDINAL* is controlled by similar regulatory networks in both species.

The subcellular location of *Cardinal* was evaluated by single-molecule RNA fluorescence *in situ* hybridization (FISH). *Cardinal* was detected in the nuclear and cytoplasmic compartments of both HL-1 cells and isolated adult mouse cardiomyocytes (Figure 1J and 1K). As a control, we confirmed that expression of Neat1, a previously reported nuclear lncRNA (27), is restricted to the nucleus (Suppl. Figure 3). Quantification showed that more than 60% of the *Cardinal* signal was in the cytoplasm in both HL-1 cells and adult cardiomyocytes (Figure 1L). To confirm the above observations, we isolated cytosolic and nuclear factions from HL-1 cells and adult cardiomyocytes and detected *Cardinal* transcripts in both (Figure 1M). Cytosolic (28s, *Gapdh*, *Hprt*) and nuclear (U6, Mhrt, Chaer, Neat1) transcripts were detected in their expected fractions (Figure 1M).

CARDINAL alters the translation rate in cardiomyocytes

We assessed the effect of *CARDINAL* on protein translation in cardiomyocytes. Global translation was assessed by surface sensing of translation (SUnSET) (28). Before harvest, cells were incubated in medium containing puromycin, which is incorporated into the nascent

polypeptide chain. Western blot of the puromycin incorporated protein reflects the amount of newly synthesized protein within a period of time (i.e., the translation rate, Figure 2A). In isolated neonatal rat ventricular cardiomyocytes (NRVCs), overexpression of *Cardinal* did not alter translation rate from the baseline under normal conditions (Figure 2B and 2C). We then tested the effect of *Cardinal* under stress conditions using Phenylephrine (PE is a hypertrophic agonist that also promotes the translation rate in cardiomyocytes) (4). As expected, an induction in the translation rate in NRVCs was observed 24 hours after stimulation with PE; this PE-induced enhancement was suppressed by adenovirus-mediated overexpression of *Cardinal* (Figure 2B and 2C). This observation was further supported using the FlUorescent Non–Canonical Amino acid Tagging (FUNCAT) assay (Figure 2D and 2E). Since *Cardinal* is highly expressed in adult hearts, we also attempted to evaluate its effect on translation in isolated adult cardiomyocytes. As observed with the NRVCs, *Cardinal* was able to suppress the PE-induced translational increase (Figure 2F and 2G). These data support a role for *CARDINAL* as a potent suppressor of translation in cardiomyocytes.

Ribosome-bound *CARDINAL* is increased in cardiac hypertrophy

Since increased translation is a major observation during cardiac hypertrophy, we asked whether the level of *CARDINAL* was altered during this process. We first analyzed transcriptomic data from more than 300 human heart samples and found that the level of *CARDINAL* was increased in human failing hearts regardless of its etiology (Figure 3A). We validated these results by RT-qPCR using human diseased heart samples (Figure 3B). Similarly, *Cardinal* was increased in a mouse model of pressure-overload induced cardiac hypertrophy (Figure 3C). *Cardinal* expression was also dramatically increased in hearts isolated from

Calcineurin A (*CnA*) transgenic mice (Figure 3D); the cardiac hypertrophy induced by *CnA* overexpression is also associated with elevation of the hypertrophic markers *Bnp* and *Myh7* (29). As further support, an increased level of *Cardinal* was observed in isolated adult cardiomyocytes treated with PE to induce hypertrophy (Figure 3E).

To better understand how the transcription of the *CARDINAL* gene is induced during cardiac hypertrophy, we examined the promoter regions of the *CARDINAL* gene. Pressure-overload induced cardiac hypertrophy was associated with increased H3K9 acetylation at the promoter regions of *Cardinal*, indicating active transcription of *Cardinal* during cardiac hypertrophy (Figure 3F). As a positive control, we observed that *Anp* genomic locus was also activated (Figure 3F). The sequences of these promoters were analyzed by the Find Individual Motif Occurrences tool to identify potential transcription factor binding sites at these regions (30). Analyses of the promoter sequences from both mouse and human genomes found multiple overlapping and conserved transcription factor binding sites, which included those for myocyte enhancer factor-2 (MEF2) and nuclear factor of activated T-cells (NFAT) (Figure 3G), two important transcription factors that mediate transcriptomic changes in the heart under normal conditions and during cardiac hypertrophy (5). The binding of MEF2 to the promoter sequence was validated by MEF2A CHIP-seq (Figure 3H). The results were consistent with the regulatory role of MEF2 on *CARDINAL* expression as previously reported (22). *CnA*-Tg mice (transgenic line where the Myh6 promoter drives expression of a constitutively active Calcineurin A (Ppp3ca) cDNA in cardiomyocytes) have sustained activated NFAT activity in heart (29); coupled with the dramatic increase of *Cardinal* expression in *CnA*-Tg hearts (Figure 3D), this further supports a role for NFAT activated *CARDINAL* transcription.

We next asked whether the increased *CARDINAL* expression correlated with an increased association with the ribosome during heart failure. We used cardiomyocyte specific Ribosome sequencing (Ribo-seq) data to identify transcript fragments protected by ribosomes (31); our analysis revealed that ribosome protected *Cardinal* began to increase 2 days after TAC surgery and peaked at 2 weeks (Figure 3I). In contrast, the overall *Cardinal* level (as revealed by RNA-seq) began to increase as early as 3 hours after TAC and peaked at 2 days (Figure 3I). Collectively, these data demonstrated that transcript level of *CARDINAL* and its association with ribosome are dynamically regulated during cardiac hypertrophy.

Loss of *CARDINAL* aggravates pressure-overload induced cardiac hypertrophy

To define the function of *CARDINAL* on translation and cardiac hypertrophy *in vivo*, we generated *Cardinal* knock-out (KO) mice (Suppl. Figure 4-6). *Cardinal*-KO completely abolished *Cardinal* expression; however, the expression of Myocardin (*Myocd*), located at a nearby locus, was not affected in the heart of *Cardinal*-KO mice (Suppl. Figure 7A). No overt phenotype was observed in young adult *Cardinal*-KO mice under normal physiological conditions (Suppl. Figure 7B and 7C and Suppl. Table 1). Next, we performed TAC surgery in control and *Cardinal*-KO mice. Similar to previous results, expression of *Cardinal* increased in Ctrl;TAC compared with Ctrl;Sham (Figure 4A). This procedure induced more cardiac hypertrophy in *Cardinal*-KO mice over that observed in TAC treated control animals (Figure 4B-4I). Compared with Ctrl;TAC, *Cardinal*-KO;TAC also had further increased ventricular weight/body weight (Figure 4B), heart size (Figure 4C), and cardiomyocyte cross-sectional area (Figure 4D and 4E). We also observed an increase in cardiac fibrosis in *Cardinal*-KO;TAC hearts (Figure 4F and 4G). Furthermore, the expression levels of the hypertrophic markers *Anp*,

Bnp, and *Acta1*, and the fibrosis marker *Fbn1*, are all further induced in *Cardinal*-KO;TAC hearts (Figure 4H). Echocardiographic measurement showed that control mice developed cardiac hypertrophy under TAC conditions; however, we observed further decompensated remodeling and worsened cardiac function in *Cardinal*-KO;TAC hearts (Figure 4I and Suppl. Table 2). To further demonstrate the regulatory function of *CARDINAL* in cardiac hypertrophy *in vivo*, titrated ectopic expression of *Cardinal* in KO hearts was achieved by adeno-associated virus to a level comparable to that in control hearts (Suppl. Figure 8A-8B). This ectopic *Cardinal* expression was able to rescue the severe cardiac hypertrophy phenotype in *Cardinal*-KO;TAC hearts (Suppl. Figure 8C-8K).

To determine the molecular pathways in the heart affected by *CARDINAL* in response to stress, we performed RNA-seq with heart samples from both control and *Cardinal*-KO mice that underwent sham or the TAC procedure. Pressure overload induced dramatic transcriptomic changes in heart, while *Cardinal*-KO further amplified these changes (Suppl. Figure 9A and 9B and Suppl. Table 3). Gene Set enrichment analysis of *Cardinal*-KO;TAC vs. Ctrl;TAC found that pathways associated with fibrosis and inflammation were upregulated, while pathways associated with fatty acid and amino acid metabolism and energy production were downregulated (Suppl. Figure 9C). These data support the hypothesis that *CARDINAL* participates in the regulation of cardiac hypertrophy in response to stress.

We wanted to confirm that *CARDINAL* affects protein translation in hypertrophic hearts in response to stress; we have already observed an increased rate of protein translation in *Cardinal*-KO hearts compared to controls 2 weeks after TAC surgery (Figure 4J and 4K). Therefore, we isolated adult cardiomyocytes from control and *Cardinal*-KO hearts, then treated

them with PE to induce cardiomyocyte hypertrophy. PE exposure boosted protein translation in these cells (Figure 4L and 4M). Upon PE stimulation, cardiomyocytes from *Cardinal*-KO mice had an even higher protein translation rate compared with those from controls (Figure 4L and 4M). Together, these data demonstrate that loss of *CARDINAL* promotes protein translation and cardiomyocyte hypertrophy in response to stresses.

Next, we wanted to explore how the translation enhancement in KO;TAC affected the proteomics in hearts. We performed quantitative mass spectrometry using heart tissues from KO;TAC vs. Ctrl;TAC mice. GSEA analysis showed that proteins related to actin and cytoskeleton organization, fibrosis, endoplasmic stress, and inflammation were upregulated, with the term "actin filament organization" on the top. Proteins related to energy production and metabolism were downregulated (Figure 4N). In contrast, "actin filament organization" was not among the top terms in the list of upregulated genes from the original GSEA analysis of transcriptomic changes in KO;TAC hearts (Suppl. Figure 9C). The differences in these two GSEA analyses suggest that the upregulation of "actin filament organization" proteins is likely caused by the increase in translation. In parallel, we performed Ribo-seq using hearts in KO;TAC vs. Ctrl;TAC. Consistently, the GSEA analysis of Ribo-seq data revealed an upregulation of "actin filament organization" genes (Figure 4O), suggesting *Cardinal*-KO promoted the translation of these genes in cardiomyocytes. Consistent with previous report, upregulation of "actin filament organization" proteins are closely linked to the promotion of cytoskeleton remodeling in cardiomyocytes, which is one of the core mechanisms for inducing cardiac hypertrophy (32). As expected, our analysis further showed that multiple upregulated proteins in the "actin filament organization" gene set have been documented as pro-

hypertrophic factors (Figure 4P) (33-44).

CARDINAL overexpression attenuates cardiac hypertrophy

Since loss of *CARDINAL* in the heart led to an increase in cardiac hypertrophy under stress conditions, we next investigated if overexpression of *CARDINAL* could suppress cardiac hypertrophy. We cloned the full-length mouse *Cardinal* sequence into a vector containing adeno-associated virus, serotype 9 (AAV9) with a cardiomyocyte specific cTNT promoter, to generate AAV9-cTNT-*Cardinal* virus. Mice injected with AAV9-cTNT-*Cardinal* virus (either AAV9-cTNT-*GFP* or AAV9-cTNT-*Cardinal-antisense* virus used as control) were subjected to TAC or sham surgery (Figure 5A and Suppl. Figure 10). RT-qPCR was used to confirm the sustained overexpression of *Cardinal* throughout adulthood (Figure 5B). Cardiac-specific *Cardinal* overexpression did not result in an overt phenotype under normal physiological conditions. However, while control mice developed pathological cardiac hypertrophy 4 weeks after TAC surgery, cardiomyocyte-specific overexpression of *Cardinal* suppressed these changes (Figure 5C-5K and Suppl. Figure 10). Compared with AAV9-*GFP*;TAC group, *Cardinal* overexpressing mice demonstrated a decrease in ventricular weight/body weight ratio (Figure 5C), a smaller heart size (Figure 5D, 5E) and reduced cardiomyocyte cross-sectional area (Figure 5F, 5G), a decreased fibrotic area (Figure 5H, 5I), lower expression levels of the hypertrophic markers *Anp*, *Bnp*, *Acta1*, and the fibrosis marker fibronectin (*Fn*) (Figure 5J), and improved cardiac function (Figure 5K and Suppl. Table 4). These data demonstrate the potential of *CARDINAL* overexpression in treating pressure-overload induced cardiac hypertrophy.

To further evaluate the effect of *CARDINAL* on cardiomyocyte hypertrophy, we used an *in*

vitro cardiomyocyte hypertrophy model. PE stimulation led to increased cardiomyocyte size in NRVCs, which was suppressed upon Ad-*Cardinal* treatment (Figure 5L-5M). PE-induced expression of the hypertrophic markers *Anp*, *Bnp*, and *Acta1* was also repressed by *Cardinal* (Figure 5N). Together, the *in vivo* and *in vitro* data support the potential of *CARDINAL* overexpression for the attenuation of cardiomyocyte hypertrophy.

CARDINAL interacts with the translational regulator DRG1

We hypothesized that *CARDINAL* functions by interacting with proteins associated with the ribosome and influencing protein translation. In order to understand the molecular mechanism of *CARDINAL* function and to identity its interacting proteins, we performed RNA pull-down experiments, followed by mass spectrometry. We performed these experiments in three independent conditions/settings to increase the specificity (Figure 6A). We used an *in vitro* transcribed *Cardinal* probe labeled with biotin to pull down proteins from adult mouse hearts (Set 1). Similarly, we used an *in vitro* transcribed *Cardinal* probe labeled with biotin to pull down proteins from neonatal mouse hearts (Set 2). And finally, we used a biotin labeled DNA probe complementary to *Cardinal* to pull-down proteins from a lysate of HL-1 cells (Set3). These three approaches yielded a single shared protein, Developmentally Regulated GTP Binding Protein 1 (DRG1) (Figure 6B and Suppl. Tables 5-8).

DRG1 has been implicated in a variety of biological functions, including an association with the polysome to regulate protein translation (45, 46). We verified the interaction of *Cardinal* and DRG1 using RNA immunoprecipitation (RIP) followed by RT-qPCR (Figure 6C). Additionally, we performed RNA pull-down followed by western blotting to confirm the interaction between *Cardinal* and DRG1 (Figure 6D). Endogenous DRG1 RIP in HL-1 cells

also resulted in *Cardinal* enrichment (Figure 6E). As a control, the *Cardinal* antisense (*Cardinal-as*) and an unrelated lncRNA Linc-p21 did not interact with DRG1 (Figure 6C and Suppl. Figure 11A and 11B). Interestingly, a recent study found that DRG1 suppressed ribosomal stalling on mRNA, therefore promoting efficient translation (46). To better understand the function and mechanism of DRG1 in cardiomyocytes, we performed DRG1 protein pull down in neonatal cardiomyocytes, followed by mass spectrometry. Proteins enriched in precipitate pulled down by DRG1 compared with the negative control were considered DRG1-interacting proteins; a known DRG1 partner DFRP1 was pulled down by DRG1 but not the negative control, demonstrating the efficacy of the assay (Suppl. Table 9).

We found that a large sub-set of DRG1-interacting proteins were ribosome-associated components (Suppl. Figure 11C and 11D and Suppl. Table 9). While this result provides further support that DRG1 may mediate ribosome activity and protein translation in the heart, ribosomal proteins are a common contaminant in IP-MS/MS studies. The control construct (Ad-GFP) was included for comparison to ensure the specificity of the interaction of these proteins with DRG1, as previously described for DFRP1. In addition, we found that during cardiac hypertrophy induced by TAC surgery, there was a dramatic increase in the ribosome footprints near the start codon of *Myh7*, a transcript expressed in the ventricular wall that is dramatically induced during cardiac hypertrophy (Figure 6F). These results suggest that regulation of ribosome stalling is a possible mechanism for the translational changes observed during cardiac hypertrophy.

To directly test the function of DRG1 during translation, we knocked down *Drg1* in HL-1 cardiomyocytes and observed a decrease in protein translation (Figure 6G and 6H). We also

determined that *Drg1* knock-down suppressed the PE-induced increase in translation rate in NRVCs (Figure 6I and 6J), resulting in reduced cardiomyocyte size and decreased expression of hypertrophic markers *Anp* and *Bnp* (Figure 6K-6M). Based on these results, we propose a role for DRG1 in cardiac hypertrophy; specifically, our data support a model in which the lncRNA *CARDINAL* and ribosomal protein DRG1 interact to regulate protein translation during cardiac hypertrophy.

The presented data suggested that *CARDINAL* might regulate ribosome stalling in cardiac hypertrophy. Previously, multiple conserved amino acid motifs have been reported to be tightly associated with the occurrence of ribosome stalling (47). When we compared the upregulated proteins with the other proteins identified by the mass spectrometry analyses, stalling motifs were enriched in upregulated proteins both in terms of motif categories and motif number (Figure 6N and 6O). The results suggested that loss of *CARDINAL* led to suppression of ribosome stalling.

Next, we asked why the translation of proteins related to "actin filament organization" were specifically enhanced. A similar analysis of stalling motifs showed that they were enriched in "actin filament organization" proteins both in terms of motif categories and motif number (Figure 6P and 6Q). These results further suggest that translation of "actin filament organization" proteins are more likely affected by ribosome stalling, and therefore, more translation of "actin filament organization" genes occurred in *Cardinal*-KO stressed hearts due to the suppression of ribosome stalling via DRG1.

CARDINAL destabilizes DRG1 by preventing its interaction with DFRP1

To better understand the molecular mechanisms underlying the observed *CARDINAL*-

DRG1 interaction and their function in cardiac hypertrophy, we further examined the expression and function of DRG1 protein in hypertrophic cardiomyocytes. In NRVCs, PE treatment increased the amount of DRG1 protein, which was attenuated by *Cardinal* overexpression (Figure 7A and 7B). However, *Cardinal* overexpression did not affect the mRNA level of *Drg1* transcripts (Figure 7C). DRG1 protein level was also increased in TAC-stressed hearts, and further increased in *Cardinal*-KO hearts after the TAC procedure (Figure 7D and 7E); as with the PE treatment, there was no observed change in *Drg1* mRNA levels in *Cardinal*-KO hearts when compared to control (Figure 7F). In contrast, *Cardinal* overexpression in cardiomyocytes suppressed the increase of DRG1 protein in the TAC-stressed heart (Figure 7G and 7H). These data revealed an inverse correlation between the expression pattern of the *Cardinal* transcript and DRG1 protein level in cardiomyocytes in response to stress.

DFRP1 is an interacting partner of DRG1, which stabilizes DRG1 protein via their direct interaction (48). We first tested whether changes in DRG1 protein level resulted from changes in DFRP1 protein level. However, *Cardinal* knock-out or overexpression did not result in obvious changes in DFRP1 level after either sham or TAC (Figure 7G, Suppl. Figure 12A-C). Therefore, we hypothesized that *CARDINAL* downregulates DRG1 protein level by interfering with its interaction with DFRP1. We first validated the interaction between DRG1 and DFRP1 by both exogenous and endogenous co-immunoprecipitation (co-IP) (Figure 7I and 7J). Overexpression of *Dfrp1* increased the amount of DRG1 protein (Figure 7K), consistent with a previous report showing that DFRP1 stabilizes DRG1 protein (48). As expected, *Cardinal* overexpression inhibited the effect of DFRP1 on DRG1 protein level in a dose-dependent

manner (Figure 7K), but it did not affect DRG1 protein level in the absence of DFRP1 (Suppl. Figure 12D). Next, we tested the effect of *Cardinal* on the interaction between DRG1 and DFRP1 by co-IP and demonstrated that co-IP in the presence of *Cardinal* attenuated the interaction between DRG1 and DFRP1 proteins (Figure 7L). As a control, overexpression of *Cardinal-as* did not affect DRG1-DFRP1 interaction (Suppl. Figure 12E). We further tested this finding using endogenous co-IP. A stable knock-down of *Cardinal* in HL-1 cells and control HL-1 lines were generated (Figure 7M). With less *Cardinal*, the interaction between DRG1 and DFRP1 became stronger (Figure 7N). In order to test whether DRG1 is required for *CARDINAL* to influence protein translation and cardiac hypertrophy, we assessed its activity upon *Drg1* knock-down. Both *Cardinal* overexpression and *Drg1* knock-down decreased protein translation in NRVCs under the treatment of PE (Figure 7O and 7P). However, *Cardinal* overexpression in conjunction with *Drg1* knock-down did not further inhibit translation (Figure 7O and 7P). This result supports a model for the inhibition of protein translation by *CARDINAL* through the downregulation of DRG1 protein levels.

Discussion

Here, we report the function of the cardiac-specific lncRNA *CARDINAL* in cardiac hypertrophy and protein translation. We found that *CARDINAL* modulates the process of translation and cardiac hypertrophy in response to stress by restraining the level and function of the translation regulator DRG1. We further demonstrated that the level of DRG1 protein and its interaction with DFRP1 are increased under pathophysiological stress conditions; as a result, translational elongation is enhanced, increasing overall protein translation, and inducing cardiac hypertrophy. Genetic deletion of *Cardinal* facilitates more stable formation of the DRG1-DFRP1 complex, enhanced protein translation, and thereby, cardiac hypertrophy. Our data reveal that the lncRNA *CARDINAL* regulates hypertrophic remodeling primarily under stress conditions (Figure 8). These findings further support the view that many lncRNAs are not essential for normal development or physiological function; instead, they are critical regulators for stress responses.

Translation enhancement is one of the distinct features of cardiac hypertrophy(4); modulating this biological process is effective in suppressing cardiac hypertrophy (9-11). However, as translation is a basic cellular function in all cell types, organism-wide inhibition of translation leads to serious side effects. The fact that the heart has one of the lowest protein synthesis rates among different tissues compounds the problem (49). The harmful influence of inhibiting translation globally would outweigh any beneficial effect observed in a single tissue or cell type. Since many lncRNAs have higher tissue specificity than protein coding genes, a cardiac-specific lncRNA with the ability to regulate ribosomal activity could facilitate a targeted therapy to treat cardiac hypertrophy.

Since lncRNAs do not have protein coding potential, they were not originally expected to be associated with the ribosome or to participate in protein translation. However, multiple translatomics techniques, including Ribo-seq (19, 31), Translating Ribosome Affinity Purification (TRAP)-seq (21), and RNA-seq of polysome fractions from polysome profiling (25, 50), indicated this was not the case and association was common; however, the biological implications of this association was not immediately understood (19). In this study, we identified a cardiac-specific ribosome associated lncRNA, *CARDINAL*, that influences protein translation. We provide evidence that this ribosome-associated lncRNA can affect ribosomal function and protein translation and, in turn, alter the severity of cardiac hypertrophy. Our study describes a promising therapeutic target for "translation-based" therapy of heart failure and also emphasizes the potential translation-regulatory role of ribosome associated lncRNAs.

CARDINAL was previously identified by Anderson et al. and described to have a role in transcriptional regulation (22). They demonstrated that *CARDINAL* functioned in the nucleus by interacting with SRF. The investigators also demonstrated that the *Cardinal*-KO exacerbated systolic dysfunction after myocardial infarction. While our data also confirmed the nuclear localization of *Cardinal*, we found that it is more highly abundant in the cytoplasm of cardiomyocytes. We then demonstrated an interaction between *CARDINAL* and the ribosome in the cytoplasmic compartment. Therefore, it appears that both nuclear and cytoplasmic *CARDINAL* are functional, although each likely acts using a different mechanism. The present study reveals an important function for *CARDINAL* in altering ribosomal function and consequently, cardiac hypertrophy.

The first report describing DRG1 was published over 30 years ago (51). The most

established feature of DRG1 is its association with ribosome (48, 52). However, its molecular role in protein synthesis was not known until a recent study was published describing its function in yeast (46); the authors found that the attachment of DRG1 to ribosomes promoted efficient translation by suppressing ribosome stalling (46). When a translating ribosome meets a stall signal on a mRNA, it transforms into an "unproductive" conformation (53). The authors proposed that the binding of DRG1 stabilized the ribosome in a "productive" conformation that was competent to proceed further in the elongation cycle (46). Our study linked DRG1 to cardiac hypertrophy and demonstrated that the upregulation of DRG1 protein was, at least partially, responsible for the enhancement of translation observed during cardiac hypertrophy. It also functions as a downstream target of *CARDINAL* in the regulation of ribosomal function. These data demonstrate that the ribosome is a highly dynamic organelle that is regulated by a complex network, especially during the development of cardiac hypertrophy. However, the details regarding the mechanism of *CARDINAL* function in ribosome stalling still need further elucidation. It will also be interesting to explore whether the suppression of ribosome stalling in *Cardinal*-KO hearts leads to compromised protein quality control.

In summary, our study identified a cardiac-specific ribosome associated lncRNA (*CARDINAL*). *CARDINAL* suppresses the increase in translation observed during cardiac hypertrophy and the associated pathology. *CARDINAL* suppressed upregulation of DRG1 protein levels during cardiac hypertrophy by preventing its interaction with its stabilizing partner DFRP1. This study highlights an important role for this lncRNA in the protein translation of cardiomyocytes and provides a feasible therapeutic target to treat cardiac hypertrophy by specifically modulating ribosomal function in the heart.

Methods

Sex as a biological variable.

For experiments involving human subjects, our study examined tissue from both males and females and similar findings are reported for both sexes. For experiments involving mice, our study examined only male animals since they exhibited less variability in phenotype.

Human samples

Left ventricular (LV) tissues were collected from patients with dilated cardiomyopathy (DCM) during heart transplantation performed in the First Affiliated Hospital of Sun Yat-sen University. When diseased hearts were removed from patients, a piece of LV tissue was dissected and snap-frozen in liquid nitrogen. LV tissue from donors who died for noncardiac reasons were used as control. All procedures conformed to the 1964 Helsinki declaration and its later amendments or comparable ethical standards and approved by the Ethics Committee of the First Affiliated Hospital of Sun Yat-sen University, Guangzhou, China.

Animal models

Cardiac hypertrophy was induced by transverse aortic constriction (TAC) surgery as described previously (54). Mice with a body weight of 25-30g were anesthetized with isoflurane (3%–4% isoflurane for induction, 1%–2% isoflurane for maintenance). The chest was shaved and disinfected with alcohol. The chest was opened by left second intercostal thoracotomy. A 26-gauge needle was put on the ascending aorta. The needle and the ascending aorta were tightly ligated together using a 7-0 nylon suture at the transverse aorta, and the 26-gauge needle was removed immediately after ligation. In the sham operation, all procedures were the same except that no ligation was performed. Dissected intercostal space and chest

skin were closed using a 6-0 silk suture. Mice genotypes were blinded to the surgeon. Cardiac hypertrophy was assessed 4 weeks after surgery. *CnA*-Tg mice (Tg(Myh6-Ppp3ca)37Eno/J), were obtained from the Jackson Laboratory (Strain #:009075). In this strain, the Myh6 promoter drives expression of a constitutively active Calcineurin A (Ppp3ca) cDNA in cardiomyocytes, serving as another model for cardiac hypertrophy,

Statistics

Mean and standard deviation were presented for each measurement, unless otherwise stated. Normality of data was evaluated by the Shapiro–Wilk test where warranted. For comparison between 2 groups, a Student's t-test was performed if the variable followed normal distribution, while a Mann-Whitney U test was performed if it did not follow a normal distribution. For comparison among multiple groups, either 1-way or 2-way (if there were 2 factor levels) ANOVA was performed for variables with normal distribution, otherwise a Kruskal-Wallis H test was performed. For pairwise comparisons, post-hoc tests were performed with Tukey's correction. Values of $p<0.05$ were considered statistically significant.

Study approval

All animal experiments were approved by Independent Ethics Committee for Clinical Research and Animal Trials of the First Affiliated Hospital of Sun Yat-sen University (protocol# [2019]018) and the Institutional Animal Care and Use Committees (IACUCs) at Boston Children's Hospital (protocol# 18-08-3759R) and the University of South Florida (protocol# IS00009392).

The detailed experimental methods are available in Supplementary Methods. Sequences of primers used in this study for RT-qPCR are summarized in Suppl. Table 10.

Data availability

Supporting data values associated with graphs in the main manuscript and supplemental material are provided in a single Excel (XLS) file entitled “Supporting data values”. Values for each figure are presented in separate tabs.

Next-generation sequencing data generated in this study have been deposited in public databases. Genome Sequence Archive in National Genomics Data Center of Chinese Academy of Sciences (https://ngdc.cncb.ac.cn/gsa; GSA: CRA014575) for Ribo-seq; Gene Expression Omnibus (GEO) in NCBI (https://www.ncbi.nlm.nih.gov/geo/; GSE210985) for RNA-seq. Values for all data points in graphs can be found in the file of Supplemental Supporting data values.

Author contributions

Z.-P.H., D.-Z.W. and J.H. conceived the project, designed, and analyzed the experiments, and wrote the manuscript. X.H., T.Y. and Y.W.L. performed molecular biology experiments and collected most of the data. H.Z., T.L. and Y.Y. contributed to human sample acquisition and western blotting analysis. G.D. and Q.M. performed transverse aortic constriction surgery and collected mouse heart samples. C.L. contributed to the echocardiographic data acquisition and analysis. M.Z. and Z.L. contributed to the histological and immunofluorescent data acquisition and analysis. G.W. contributed to bioinformatic analyses of deep sequencing data. H.C., W.P., Y.D. and J.O. supervised the *Cardinal*-KO mice generation and surgery. H.C., W.P., Y.D., J.O., and J.D.M. reviewed and edited the manuscript. The determination of first author order was made based on each individual's contribution to the figures and writing of the manuscript.

Acknowledgements

We thank members of the Huang and Wang laboratory for advice and support. This work is supported by National Key R&D Program of China (2021YFA1302500), National Natural Science Foundation of China (U23A20396 and 82270252 to Z.-P.H. and 82370382 to X.H.), Guangzhou Municipal Science and Technology Bureau (202206010139 to Z.-P.H.), Guangdong Basic and Applied Basic Research Foundation (2019B151502003 to Z.-P.H.), Additional Ventures (Grant 1014383 to D.-Z.W.) and National Institutes of Health (R01HL149401, R01HL138757, R01HL165794, and R01HL168900 to D.-Z.W.)

Conflicts of interest

The authors declare no competing interests.

References

1. Conrad N, Judge A, Tran J, Mohseni H, Hedgecott D, Crespillo AP, et al. Temporal trends and patterns in heart failure incidence: a population-based study of 4 million individuals. *Lancet.* 2018;391(10120):572-80.
2. Taylor CJ, Ordonez-Mena JM, Roalfe AK, Lay-Flurrie S, Jones NR, Marshall T, et al. Trends in survival after a diagnosis of heart failure in the United Kingdom 2000-2017: population based cohort study. *BMJ.* 2019;364:l223.
3. Nakamura M, and Sadoshima J. Mechanisms of physiological and pathological cardiac hypertrophy. *Nat Rev Cardiol.* 2018;15(7):387-407.
4. Wang Y, Zhang Y, Ding G, May HI, Xu J, Gillette TG, et al. Temporal dynamics of cardiac hypertrophic growth in response to pressure overload. *Am J Physiol Heart Circ Physiol.* 2017;313(6):H1119-H29.
5. He X, Du T, Long T, Liao X, Dong Y, and Huang ZP. Signaling cascades in the failing heart and emerging therapeutic strategies. *Signal Transduct Target Ther.* 2022;7(1):134.
6. Schwanhausser B, Busse D, Li N, Dittmar G, Schuchhardt J, Wolf J, et al. Global quantification of mammalian gene expression control. *Nature.* 2011;473(7347):337-42.
7. Yan Y, Tang R, Li B, Cheng L, Ye S, Yang T, et al. The cardiac translational landscape reveals that micropeptides are new players involved in cardiomyocyte hypertrophy. *Mol Ther.* 2021;29(7):2253-67.
8. Han Y, Du T, Guo S, Wang L, Dai G, Long T, et al. Loss of m(6)A Methyltransferase METTL5 Promotes Cardiac Hypertrophy Through Epitranscriptomic Control of SUZ12 Expression. *Front Cardiovasc Med.* 2022;9:852775.

9. Chorghade S, Seimetz J, Emmons R, Yang J, Bresson SM, Lisio M, et al. Poly(A) tail length regulates PABPC1 expression to tune translation in the heart. *Elife.* 2017;6:e24139.
10. Grund A, Szaroszyk M, Korf-Klingebiel M, Malek Mohammadi M, Trogisch FA, Schrameck U, et al. TIP30 counteracts cardiac hypertrophy and failure by inhibiting translational elongation. *EMBO Mol Med.* 2019;11(10):e10018.
11. Hardt SE, Tomita H, Katus HA, and Sadoshima J. Phosphorylation of eukaryotic translation initiation factor 2Bepsilon by glycogen synthase kinase-3beta regulates beta-adrenergic cardiac myocyte hypertrophy. *Circ Res.* 2004;94(7):926-35.
12. Tahmasebi S, Khoutorsky A, Mathews MB, and Sonenberg N. Translation deregulation in human disease. *Nat Rev Mol Cell Biol.* 2018;19(12):791-807.
13. McMullen JR, Sherwood MC, Tarnavski O, Zhang L, Dorfman AL, Shioi T, et al. Inhibition of mTOR signaling with rapamycin regresses established cardiac hypertrophy induced by pressure overload. *Circulation.* 2004;109(24):3050-5.
14. Shioi T, McMullen JR, Tarnavski O, Converso K, Sherwood MC, Manning WJ, et al. Rapamycin attenuates load-induced cardiac hypertrophy in mice. *Circulation.* 2003;107(12):1664-70.
15. Langin M, Mayr T, Reichart B, Michel S, Buchholz S, Guethoff S, et al. Consistent success in life-supporting porcine cardiac xenotransplantation. *Nature.* 2018;564(7736):430-3.
16. Paoletti E. mTOR Inhibition and Cardiovascular Diseases: Cardiac Hypertrophy. *Transplantation.* 2018;102(2S Suppl 1):S41-S3.
17. Li J, Kim SG, and Blenis J. Rapamycin: one drug, many effects. *Cell Metab.* 2014;19(3):373-9.

18. Cabili MN, Trapnell C, Goff L, Koziol M, Tazon-Vega B, Regev A, et al. Integrative annotation of human large intergenic noncoding RNAs reveals global properties and specific subclasses. *Genes Dev.* 2011;25(18):1915-27.
19. Guttman M, Russell P, Ingolia NT, Weissman JS, and Lander ES. Ribosome profiling provides evidence that large noncoding RNAs do not encode proteins. *Cell.* 2013;154(1):240-51.
20. van Heesch S, van Iterson M, Jacobi J, Boymans S, Essers PB, de Bruijn E, et al. Extensive localization of long noncoding RNAs to the cytosol and mono- and polyribosomal complexes. *Genome Biol.* 2014;15(1):R6.
21. Zhou P, Zhang Y, Ma Q, Gu F, Day DS, He A, et al. Interrogating translational efficiency and lineage-specific transcriptomes using ribosome affinity purification. *Proc Natl Acad Sci U S A.* 2013;110(38):15395-400.
22. Anderson DM, Anderson KM, Nelson BR, McAnally JR, Bezprozvannaya S, Shelton JM, et al. A myocardin-adjacent lncRNA balances SRF-dependent gene transcription in the heart. *Genes Dev.* 2021;35(11-12):835-40.
23. Sarropoulos I, Marin R, Cardoso-Moreira M, and Kaessmann H. Developmental dynamics of lncRNAs across mammalian organs and species. *Nature.* 2019;571(7766):510-4.
24. Pereira IT, Spangenberg L, Robert AW, Amorin R, Stimamiglio MA, Naya H, et al. Polysome profiling followed by RNA-seq of cardiac differentiation stages in hESCs. *Sci Data.* 2018;5:180287.
25. Pereira IT, Spangenberg L, Robert AW, Amorin R, Stimamiglio MA, Naya H, et al. Cardiomyogenic differentiation is fine-tuned by differential mRNA association with

polysomes. *BMC Genomics.* 2019;20(1):219.

26. van Heesch S, Witte F, Schneider-Lunitz V, Schulz JF, Adami E, Faber AB, et al. The Translational Landscape of the Human Heart. *Cell.* 2019;178(1):242-60 e29.
27. Clemson CM, Hutchinson JN, Sara SA, Ensminger AW, Fox AH, Chess A, et al. An architectural role for a nuclear noncoding RNA: NEAT1 RNA is essential for the structure of paraspeckles. *Mol Cell.* 2009;33(6):717-26.
28. Schmidt EK, Clavarino G, Ceppi M, and Pierre P. SUnSET, a nonradioactive method to monitor protein synthesis. *Nat Methods.* 2009;6(4):275-7.
29. Molkentin JD, Lu JR, Antos CL, Markham B, Richardson J, Robbins J, et al. A calcineurin-dependent transcriptional pathway for cardiac hypertrophy. *Cell.* 1998;93(2):215-28.
30. Grant CE, Bailey TL, and Noble WS. FIMO: scanning for occurrences of a given motif. *Bioinformatics.* 2011;27(7):1017-8.
31. Doroudgar S, Hofmann C, Boileau E, Malone B, Riechert E, Gorska AA, et al. Monitoring Cell-Type-Specific Gene Expression Using Ribosome Profiling In Vivo During Cardiac Hemodynamic Stress. *Circ Res.* 2019;125(4):431-48.
32. Caporizzo MA, and Prosser BL. The microtubule cytoskeleton in cardiac mechanics and heart failure. *Nat Rev Cardiol.* 2022;19(6):364-78.
33. McCalmon SA, Desjardins DM, Ahmad S, Davidoff KS, Snyder CM, Sato K, et al. Modulation of angiotensin II-mediated cardiac remodeling by the MEF2A target gene Xirp2. *Circ Res.* 2010;106(5):952-60.
34. Lu S, Crawford GL, Dore J, Anderson SA, Despres D, and Horowits R. Cardiac-specific NRAP overexpression causes right ventricular dysfunction in mice. *Experimental cell*

research. 2011;317(8):1226-37.

35. van Eldik W, den Adel B, Monshouwer-Kloots J, Salvatori D, Maas S, van der Made I, et al. Z-disc protein CHAPb induces cardiomyopathy and contractile dysfunction in the postnatal heart. *PloS one.* 2017;12(12):e0189139.
36. Abe I, Terabayashi T, Hanada K, Kondo H, Teshima Y, Ishii Y, et al. Disruption of actin dynamics regulated by Rho effector mDia1 attenuates pressure overload-induced cardiac hypertrophic responses and exacerbates dysfunction. *Cardiovasc Res.* 2021;117(4):1103-17.
37. Shi J, Zhang YW, Summers LJ, Dorn GW, 2nd, and Wei L. Disruption of ROCK1 gene attenuates cardiac dilation and improves contractile function in pathological cardiac hypertrophy. *J Mol Cell Cardiol.* 2008;44(3):551-60.
38. Shi J, Zhang YW, Yang Y, Zhang L, and Wei L. ROCK1 plays an essential role in the transition from cardiac hypertrophy to failure in mice. *J Mol Cell Cardiol.* 2010;49(5):819-28.
39. Sbroggio M, Carnevale D, Bertero A, Cifelli G, De Blasio E, Mascio G, et al. IQGAP1 regulates ERK1/2 and AKT signalling in the heart and sustains functional remodelling upon pressure overload. *Cardiovasc Res.* 2011;91(3):456-64.
40. Engelhardt S, Hein L, Keller U, Klambt K, and Lohse MJ. Inhibition of Na(+)-H(+) exchange prevents hypertrophy, fibrosis, and heart failure in beta(1)-adrenergic receptor transgenic mice. *Circ Res.* 2002;90(7):814-9.
41. Marano G, Vergari A, Catalano L, Gaudi S, Palazzesi S, Musumeci M, et al. Na+/H+ exchange inhibition attenuates left ventricular remodeling and preserves systolic function

in pressure-overloaded hearts. *Br J Pharmacol.* 2004;141(3):526-32.

42. Li Q, Song XW, Zou J, Wang GK, Kremneva E, Li XQ, et al. Attenuation of microRNA-1 derepresses the cytoskeleton regulatory protein twinfilin-1 to provoke cardiac hypertrophy. *J Cell Sci.* 2010;123(Pt 14):2444-52.
43. Li GH, Shi Y, Chen Y, Sun M, Sader S, Maekawa Y, et al. Gelsolin regulates cardiac remodeling after myocardial infarction through DNase I-mediated apoptosis. *Circ Res.* 2009;104(7):896-904.
44. Li Y, Zhang D, Kong L, Shi H, Tian X, Gao L, et al. Aldolase promotes the development of cardiac hypertrophy by targeting AMPK signaling. *Experimental cell research.* 2018;370(1):78-86.
45. Ishikawa K, Akiyama T, Ito K, Semba K, and Inoue J. Independent stabilizations of polysomal Drg1/Dfrp1 complex and non-polysomal Drg2/Dfrp2 complex in mammalian cells. *Biochem Biophys Res Commun.* 2009;390(3):552-6.
46. Zeng F, Li X, Pires-Alves M, Chen X, Hawk CW, and Jin H. Conserved heterodimeric GTPase Rbg1/Tma46 promotes efficient translation in eukaryotic cells. *Cell Rep.* 2021;37(4):109877.
47. Han P, Shichino Y, Schneider-Poetsch T, Mito M, Hashimoto S, Udagawa T, et al. Genome-wide Survey of Ribosome Collision. *Cell Rep.* 2020;31(5):107610.
48. Ishikawa K, Azuma S, Ikawa S, Semba K, and Inoue J. Identification of DRG family regulatory proteins (DFRPs): specific regulation of DRG1 and DRG2. *Genes Cells.* 2005;10(2):139-50.
49. Garlick PJ, McNurlan MA, and Preedy VR. A rapid and convenient technique for

measuring the rate of protein synthesis in tissues by injection of [3H]phenylalanine. *Biochem J.* 1980;192(2):719-23.

50. Berulava T, Buchholz E, Elerdashvili V, Pena T, Islam MR, Lbik D, et al. Changes in m6A RNA methylation contribute to heart failure progression by modulating translation. *Eur J Heart Fail.* 2020;22(1):54-66.
51. Sazuka T, Tomooka Y, Ikawa Y, Noda M, and Kumar S. DRG: a novel developmentally regulated GTP-binding protein. *Biochem Biophys Res Commun.* 1992;189(1):363-70.
52. Daugeron MC, Prouteau M, Lacroute F, and Seraphin B. The highly conserved eukaryotic DRG factors are required for efficient translation in a manner redundant with the putative RNA helicase Slh1. *Nucleic Acids Res.* 2011;39(6):2221-33.
53. Wilson DN, and Beckmann R. The ribosomal tunnel as a functional environment for nascent polypeptide folding and translational stalling. *Curr Opin Struct Biol.* 2011;21(2):274-82.
54. Huang ZP, Kataoka M, Chen J, Wu G, Ding J, Nie M, et al. Cardiomyocyte-enriched protein CIP protects against pathophysiological stresses and regulates cardiac homeostasis. *J Clin Invest.* 2015;125(11):4122-34.

Figure 1

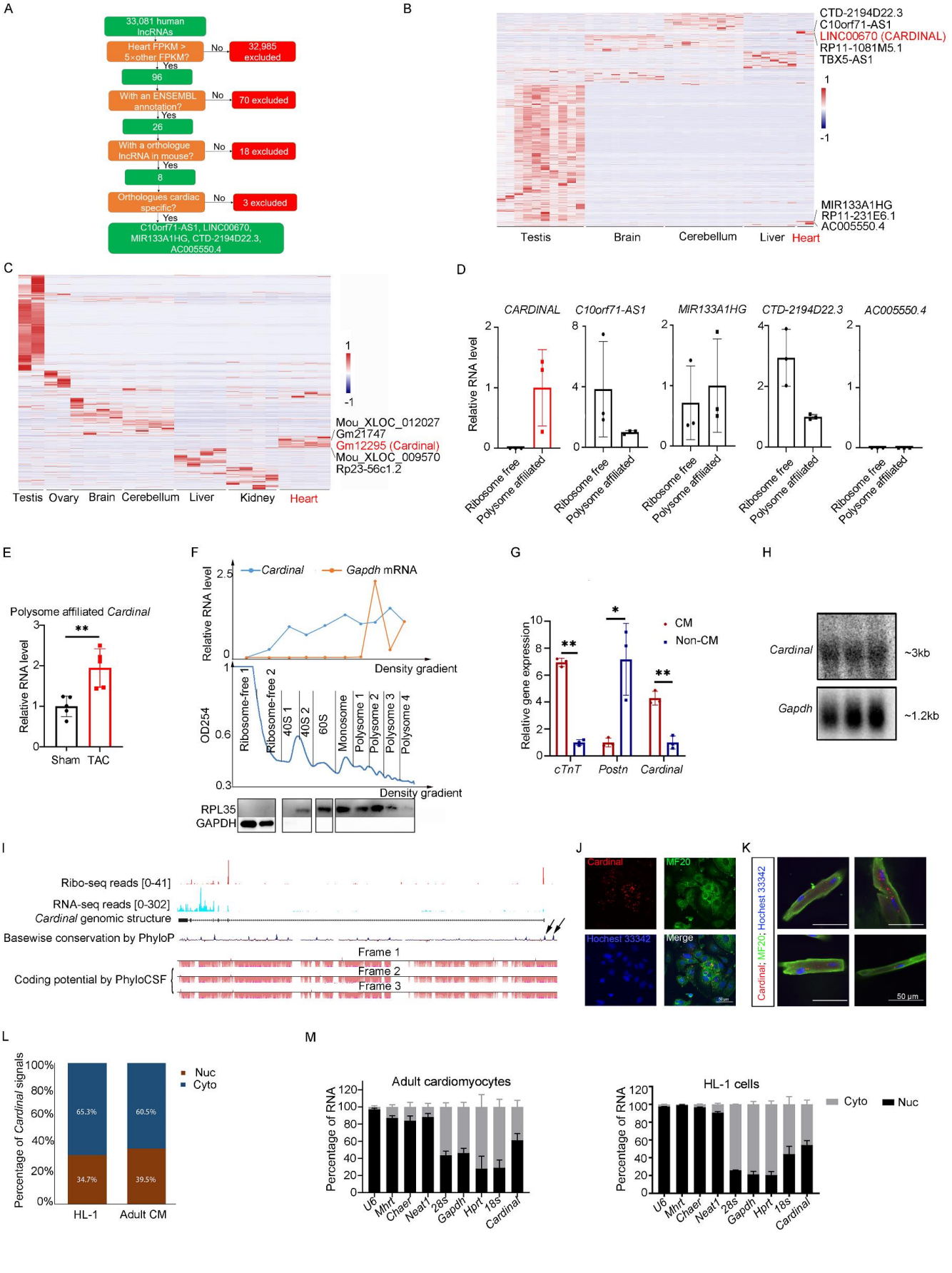
A
33,081 human lncRNAs
Heart FPKM > 5×other FPKM?
No
32,985 excluded
Yes
96
With an ENSEMBL annotation?
No
70 excluded
Yes
26
With a orthologue lncRNA in mouse?
No
18 excluded
Yes
8
Orthologues cardiac specific?
No
3 excluded
Yes
C10orf71-AS1, LINC00670, MIR133A1HG, CTD-2194D22.3, AC005550.4
B
CTD-2194D22.3
C10orf71-AS1
LINC00670 (CARDINAL)
RP11-1081M5.1
TBX5-AS1
MIR133A1HG
RP11-231E6.1
AC005550.4
Testis
Brain
Cerebellum
Liver
Heart
C
Mou_XLOC_012027
Gm21747
Gm12295 (Cardinal)
Mou_XLOC_009570
Rp23-56c1.2
Testis
Ovary
Brain
Cerebellum
Liver
Kidney
Heart
D
CARDINAL
C10orf71-AS1
MIR133A1HG
CTD-2194D22.3
AC005550.4
Relative RNA level
Ribosome free
Polysome affiliated
E
Polysome affiliated Cardinal
Relative RNA level
Sham
TAC
F
Cardinal
Gapdh mRNA
Relative RNA level
Density gradient
OD254
Ribosome-free 1
Ribosome-free 2
40S 1
40S 2
60S
Monosome
Polysome 1
Polysome 2
Polysome 3
Polysome 4
RPL35
GAPDH
G
Relative gene expression
CM
Non-CM
cTnT
Postn
Cardinal
H
Cardinal
Gapdh
~3kb
~1.2kb
I
Ribo-seq reads [0-41]
RNA-seq reads [0-302]
Cardinal genomic structure
Basewise conservation by PhyloP
Coding potential by PhyloCSF
Frame 1
Frame 2
Frame 3
J
Cardinal
MF20
Hochest 33342
Merge
K
Cardinal; MF20; Hochest 33342
50 μm
L
Percentage of Cardinal signals
Nuc
Cyto
65.3%
34.7%
60.5%
39.5%
HL-1
Adult CM
M
Adult cardiomyocytes
Percentage of RNA
U6
Mhrt
Chaer
Neat1
28s
Gapdh
Hprt
18s
Cardinal
HL-1 cells
Cyto
Nuc

Figure legends

Figure 1. Identification of *CARDINAL* by screening for cardiac-specific ribosome associated lncRNAs

A, Flow chart of screening for cardiac specific lncRNAs in a human multi-organ RNA sequencing database (https://apps.kaessmannlab.org/lncRNA_app). **B**, Heatmap showing the cardiac specificity of candidate human lncRNAs identified in panel A. **C**, Heatmap showing the cardiac specificity of mouse orthologues of candidate lncRNAs. **D**, Relative expression level of 5 lncRNA candidates detected by RNA-seq in ribosome-free fraction and polysome fraction following polysome profiling in hESC-CM (SRP150416) (N=3 for each group). **E**, Relative expression level of *Cardinal* in polysome fraction of mice hearts after sham or TAC surgery (GSE131296) (N=5 for each group). **F**, Polysome profiling of HL-1 cells and results of RT-qPCR and western blotting with different fractions. **G**, Relative expression level of *Cardinal* in different cell types in hearts detected by RT-qPCR (N=3 for each group). **H**, Northern blotting of endogenous *Cardinal* from adult mouse hearts. *Gapdh* serves as a control for loading. **I**, Genomic structure of *Cardinal* with Ribo-seq and RNA-seq reads coverage, basewise conservation calculated by PhyloP, and coding potential calculated by PhyloCSF. Black arrows indicate 2 conserved promoter regions. Tracks of Ribo-seq and RNA-seq reads coverage were obtained from http://shiny.mdc-berlin.de/cardiac-translatome/. Tracks of basewise conservation and coding potential were obtained from UCSC genome browser. **J**, Single-molecule RNA-FISH of *Cardinal* in HL-1 cells. **K**, Single-molecule RNA-FISH in cardiomyocytes from adult mice. **L**, Quantification of *Cardinal* RNA-FISH signals in nucleus and cytoplasm in at least 100 randomly selected adult cardiomyocytes and HL-1 cells. **M**,

Relative amount of *Cardinal* in nucleus vs. cytoplasm detected by RT-qPCR following nucleus/cytoplasm fractionation in adult cardiomyocytes and HL-1 cells (N=3 for each group). Statistical significance was tested by Student's T test (E and G).

Figure 2

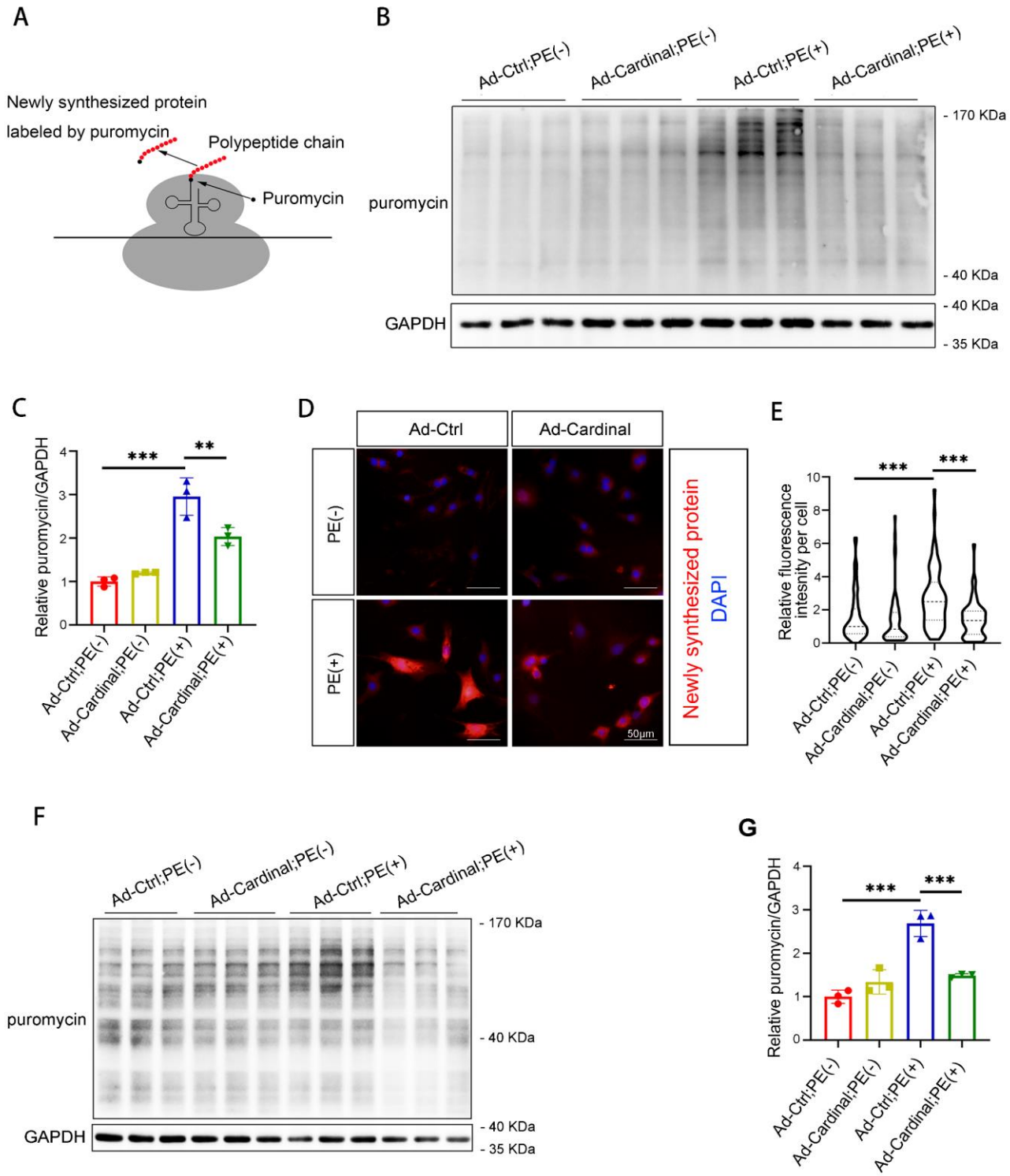
A
Newly synthesized protein
labeled by puromycin
Polypeptide chain
Puromycin
B
Ad-Ctrl;PE(-)
Ad-Cardinal;PE(-)
Ad-Ctrl;PE(+)
Ad-Cardinal;PE(+)
puromycin
GAPDH
- 170 KDa
- 40 KDa
- 40 KDa
- 35 KDa
C
Relative puromycin/GAPDH
***
**
Ad-Ctrl;PE(-)
Ad-Cardinal;PE(-)
Ad-Ctrl;PE(+)
Ad-Cardinal;PE(+)
D
Ad-Ctrl
Ad-Cardinal
PE(-)
PE(+)
Newly synthesized protein
DAPI
50μm
E
Relative fluorescence intesnity per cell
***
***
F
puromycin
GAPDH
- 170 KDa
- 40 KDa
- 40 KDa
- 35 KDa
G
Relative puromycin/GAPDH
***
***

Figure 2. *CARDINAL* modulation alters translation

A, Rationale of the SUnSET measurement. **B,** Western blotting and **C,** quantification of puromycin incorporated protein in NRVCs infected with control virus or Ad-*Cardinal* and treated by culture medium with or without PE (50μM) for 24 hours. Cells were treated by 1μM puromycin for 30 minutes before harvest. (N=3 for each group) **D,** Immunofluorescence images and **E,** fluorescence intensity quantification of NRVCs infected with control virus or Ad-*Cardinal* and treated by culture medium with or without PE (50μM) for 24 hours in FUNCAT assay. Newly synthesized protein was labeled by Alexa Fluor® 594. Violin plots were generated to show the median, 25th and 75th percentiles. At least 100 cells were measured for quantification in each group. **F,** Western blotting and **G,** quantification of puromycin incorporated protein in adult cardiomyocytes infected with control virus or Ad-*Cardinal* and treated by culture medium with or without PE (50μM) for 24 hours. Cells were treated by 1uM puromycin for 30 minutes before harvest (N=3 for each group). Statistical significance was tested by ANOVA with Tukey's post hoc test (C, E, and G).

Figure 3

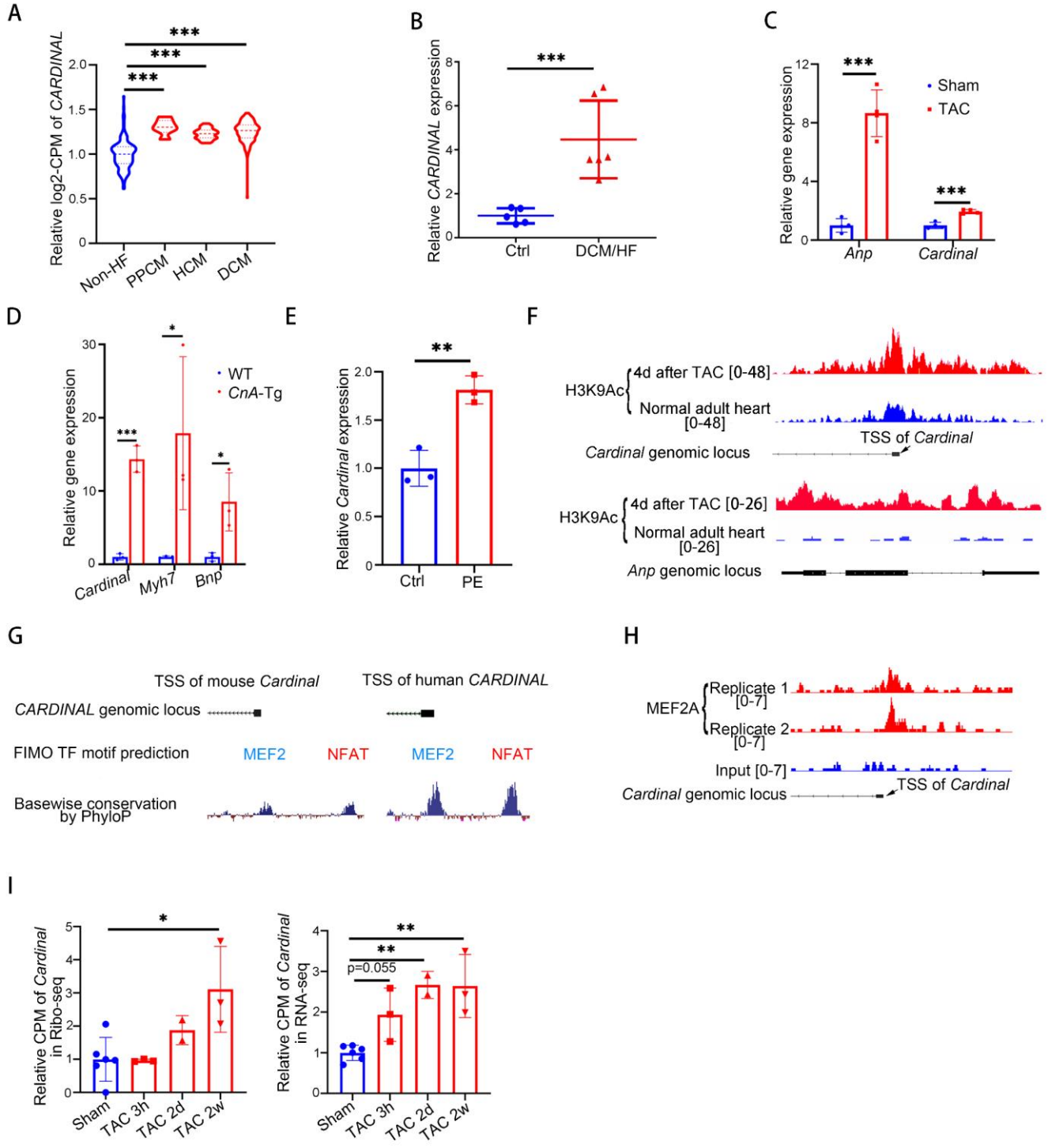
A
Relative log2-CPM of CARDINAL
***
***
***
Non-HF
PPCM
HCM
DCM
B
Relative CARDINAL expression
***
Ctrl
DCM/HF
C
Relative gene expression
***
***
Sham
TAC
Anp
Cardinal
D
Relative gene expression
WT
CnA-Tg
Cardinal
Myh7
Bnp
E
Relative Cardinal expression
**
Ctrl
PE
F
H3K9Ac
4d after TAC [0-48]
Normal adult heart [0-48]
Cardinal genomic locus
TSS of Cardinal
H3K9Ac
4d after TAC [0-26]
Normal adult heart [0-26]
Anp genomic locus
G
TSS of mouse Cardinal
TSS of human CARDINAL
CARDINAL genomic locus
FIMO TF motif prediction
MEF2
NFAT
MEF2
NFAT
Basewise conservation by PhyloP
H
MEF2A
Replicate 1 [0-7]
Replicate 2 [0-7]
Input [0-7]
Cardinal genomic locus
TSS of Cardinal
I
Relative CPM of Cardinal in Ribo-seq
*
Sham
TAC 3h
TAC 2d
TAC 2w
Relative CPM of Cardinal in RNA-seq
**
**
p=0.055
Sham
TAC 3h
TAC 2d
TAC 2w

Figure 3. Cardiac hypertrophy upregulates *CARDINAL* and enhances its association with the ribosome

A, Relative expression level of *CARDINAL* in human heart samples detected by RNA-seq from individuals without heart failure (Non-HF), with peripartum cardiomyopathy (PPCM), hypertrophic cardiomyopathy (HCM), or dilated cardiomyopathy (DCM) (GSE141910). Replicate numbers of Non-HF, PPCM, HCM, and DCM were 166, 6, 28, and 166, respectively. **B**, Relative expression of *CARDINAL* detected by RT-qPCR in human heart samples from individuals with or without heart failure (HF)/dilated cardiomyopathy (DCM) (N≥5 for each group). **C**, Relative *Anp* and *Cardinal* expression level detected by RT-qPCR in hearts 2 weeks after sham or TAC surgery (N=4 for each group). **D**, Relative expression level of *Cardinal* and hypertrophic marker *Bnp* and *Myh7* in hearts from WT or Calcineurin A transgenic mice detected by RT-qPCR (N=3 for each group). **E**, Relative *Cardinal* expression level detected by RT-qPCR in isolated adult mouse cardiomyocytes treated by culture medium with or without PE (50μM) for 24 hours. (N=3 for each group). **F**, Read coverage of histone H3K9Ac chromatin immunoprecipitation (CHIP)-seq near the transcription start site (TSS) of *Cardinal* and *Anp* from normal hearts or hearts 4 days after TAC surgery (GSE50637). **G**, MEF2 and NFAT were predicted to bind the conserved promoter regions of *CARDINAL* in both human and mouse by Find Individual Motif Occurrences (FIMO). **H**, Reads coverage of MEF2A CHIP-seq near the TSS of *Cardinal* (GSE124008). **I**, Ribosome associated and total *Cardinal* level detected by Ribo-seq and RNA-seq from hearts after sham or 3 hours, 2 days, or 2 weeks after TAC surgery (PRJNA484227). Replicate numbers of Sham, TAC 3h, TAC 2d, and TAC 2w were 6, 3, 2, 3, respectively. Statistical significance was tested by Student's T test (B, C, D, E) or ANOVA with Tukey's post hoc test (A and I).

Figure 4

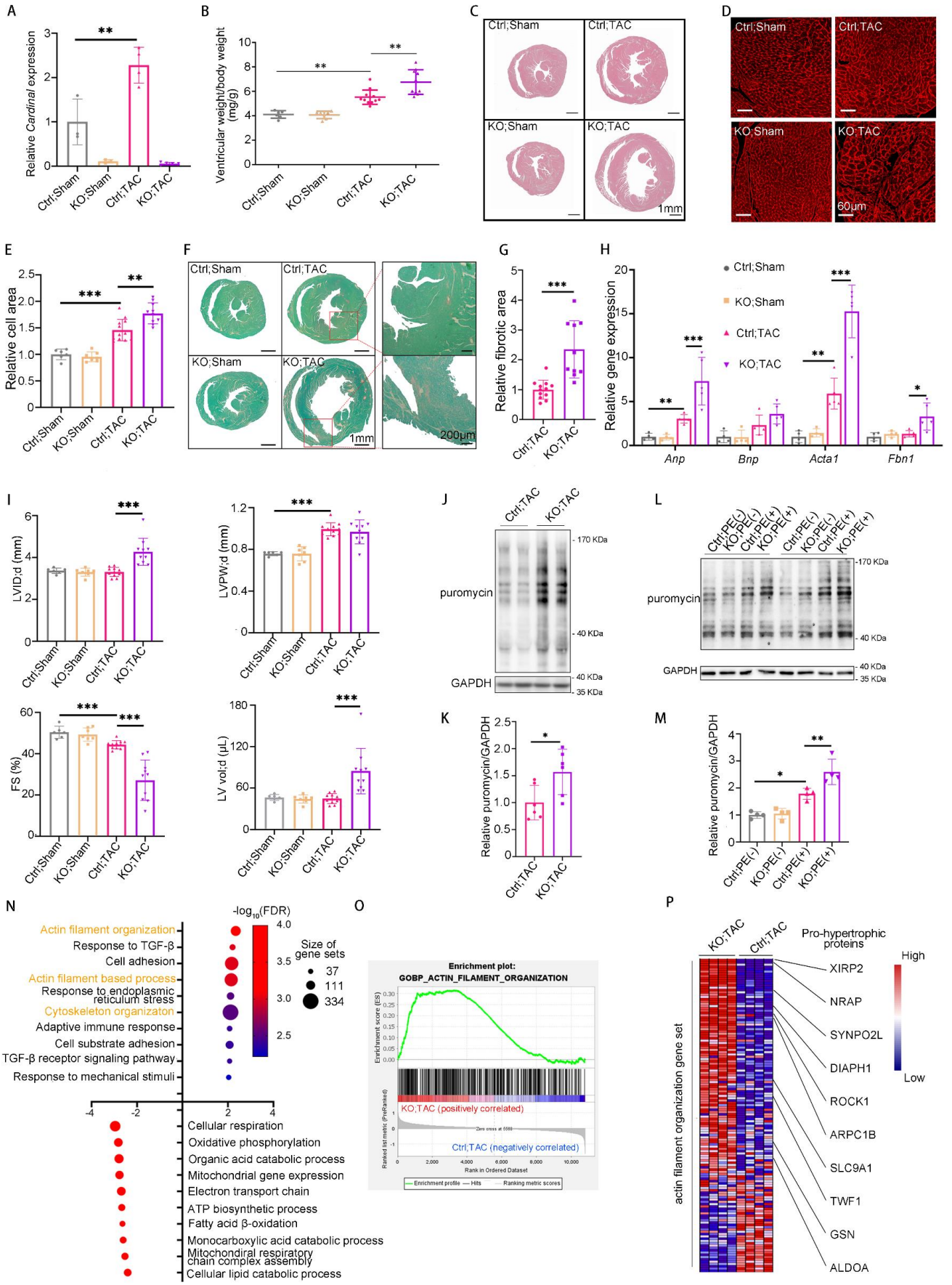
A
Relative Cardinal expression
Ctrl;Sham
KO;Sham
Ctrl;TAC
KO;TAC
B
Ventricular weight/body weight (mg/g)
C
Ctrl;Sham
Ctrl;TAC
KO;Sham
KO;TAC
1mm
D
60μm
E
Relative cell area
F
200μm
G
Relative fibrotic area
H
Relative gene expression
Anp
Bnp
Acta1
Fbn1
I
LVID;d (mm)
LVPW;d (mm)
FS (%)
LV vol;d (μL)
J
puromycin
GAPDH
170 KDa
40 KDa
35 KDa
K
Relative puromycin/GAPDH
L
Ctrl;PE(-)
KO;PE(-)
Ctrl;PE(+)
KO;PE(+)
M
N
-log10(FDR)
Size of gene sets
Actin filament organization
Response to TGF-β
Cell adhesion
Actin filament based process
Response to endoplasmic reticulum stress
Cytoskeleton organizaton
Adaptive immune response
Cell substrate adhesion
TGF-β receptor signaling pathway
Response to mechanical stimuli
Cellular respiration
Oxidative phosphorylation
Organic acid catabolic process
Mitochondrial gene expression
Electron transport chain
ATP biosynthetic process
Fatty acid β-oxidation
Monocarboxylic acid catabolic process
Mitochondiral respiratory chain complex assembly
Cellular lipid catabolic process
O
Enrichment plot:
GOBP_ACTIN_FILAMENT_ORGANIZATION
KO;TAC (positively correlated)
Ctrl;TAC (negatively correlated)
Rank in Ordered Dataset
P
Pro-hypertrophic proteins
actin filament organization gene set
XIRP2
NRAP
SYNPO2L
DIAPH1
ROCK1
ARPC1B
SLC9A1
TWF1
GSN
ALDOA
High
Low

Figure 4. Pressure-overload increases cardiac hypertrophy and enhances protein translation in *Cardinal* KO mice

A, Relative *Cardinal* expression detected by RT-qPCR (N≥3 for each group), B, ventricular weight/body weight (N≥6 for each group). **C,** H&E staining, **D,** Wheat Germ Agglutinin (WGA) staining, **E,** relative cardiomyocyte area quantification (N≥6 for each group), **F,** Sirius Red/Fast Green staining, and **G,** relative fibrosis area quantification (N≥10 for each group) performed on cross sections, **H,** relative expression level of hypertrophy and fibrosis markers detected by RT-qPCR (N≥4 for each group), and **I,** echocardiographic parameters (N≥6 for each group) of hearts from control and *Cardinal*-KO mice 4 weeks after sham or TAC surgery. **J,** Western blotting analysis and **K,** quantification of puromycin incorporated protein in hearts from control and *Cardinal*-KO mice 2 weeks after TAC surgery (N=6 for each group). Mice were peritoneally injected with 25mg/kg of puromycin 45 minutes before sacrifice. **L,** Western blotting and **M,** quantification of puromycin incorporated protein in adult mouse cardiomyocytes from control or *Cardinal*-KO mice treated by culture medium with or without PE (50μM) for 24 hours. Cells were treated by 1μM puromycin for 30 minutes before harvest (N=4 for each group). **N**, Summary of results from Gene Set Enrichment Analysis (GSEA). Proteomic changes in hearts from KO;TAC vs. Ctrl;TAC were analyzed by GSEA using the gene sets of Gene Ontology-Biological Process. **O**, Enrichment plot of the gene set "Actin Filament Organization" generated by GSEA analysis with translatomic alterations in hearts from KO;TAC vs. Ctrl;TAC. **P**, Heatmap showing proteomic changes in the "Actin Filament Organization" gene set in hearts from KO;TAC vs. Ctrl;TAC. Documented pro-hypertrophic factors among upregulated proteins were highlighted. Statistical significance was tested by Student's T test (G and K) or ANOVA with Tukey's post hoc test (A, B, E, H, I, and M).

Figure 5

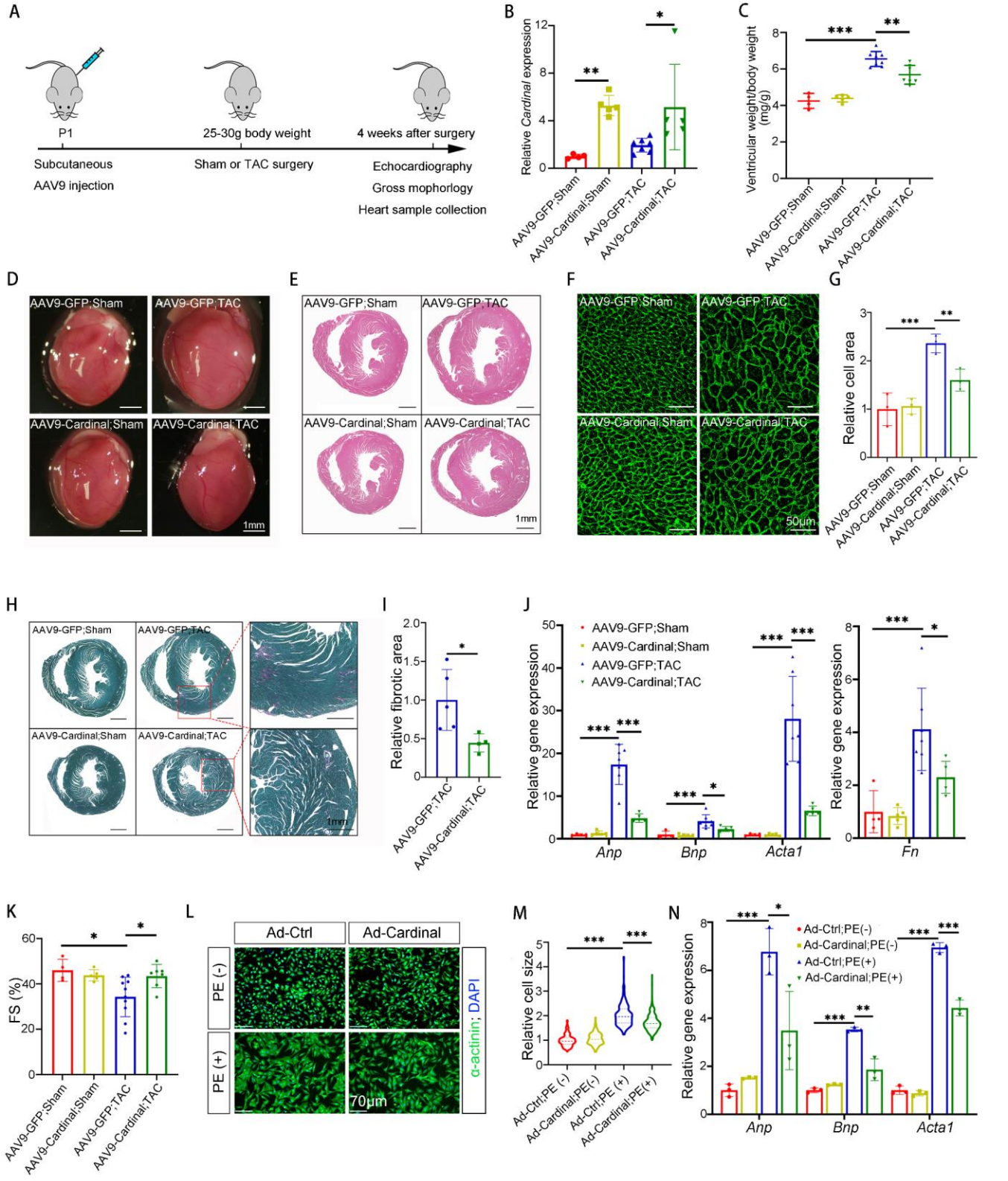
A
P1
Subcutaneous
AAV9 injection
25-30g body weight
Sham or TAC surgery
4 weeks after surgery
Echocardiography
Gross mophorlogy
Heart sample collection
B
Relative Cardinal expression
AAV9-GFP;Sham
AAV9-Cardinal;Sham
AAV9-GFP;TAC
AAV9-Cardinal;TAC
C
Ventricular weight/body weight (mg/g)
D
E
F
G
Relative cell area
H
I
Relative fibrotic area
J
Relative gene expression
Anp
Bnp
Acta1
Fn
K
FS (%)
L
Ad-Ctrl
Ad-Cardinal
PE (-)
PE (+)
α-actinin; DAPI
70μm
M
Relative cell size
Ad-Ctrl;PE(-)
Ad-Cardinal;PE(-)
Ad-Ctrl;PE(+)
Ad-Cardinal;PE(+)
N
1mm
50μm

Figure 5. *CARDINAL* overexpression attenuates cardiomyocyte hypertrophy

A, Timeline for *in vivo Cardinal* gain-of-function analysis. **B,** Relative expression of *Cardinal* (N≥4 for each group) detected by RT-qPCR. **C,** ventricular weight/body weight (N≥4 for each group), **D,** gross morphology, **E,** H&E staining, **F,** WGA staining, **G,** cardiomyocyte size quantification (N=3 for each group), **H,** Sirius Red/Fast Green staining**,** and **I,** fibrosis area quantification (N≥4 for each group) using cross sections **J,** cardiac hypertrophy and fibrosis markers (N≥4 for each group) and **K,** fraction shortening (%) of hearts from mice injected with AAV9-Ctrl or AAV9-*Cardinal* 4 weeks after sham or TAC surgery. **L,** Immunofluorescent images and **M,** cell area quantification of NRVCs infected with control virus or Ad-*Cardinal* treated using culture medium with or without PE (50μM) for 48 hours. Violin plots were generated to show the median, 25th and 75th percentiles. At least 300 cells were measured for quantification in each group. **N**, Relative expression level detected by RT-qPCR of hypertrophy markers of NRVCs infected with control virus or Ad-*Cardinal* treated using culture medium with or without PE (50μM) for 24 hours (N=3 for each group). Statistical significance was tested by Student's T test (I) or ANOVA with Tukey's post hoc test (B, C, G, J, K, M, and N).

Figure 6

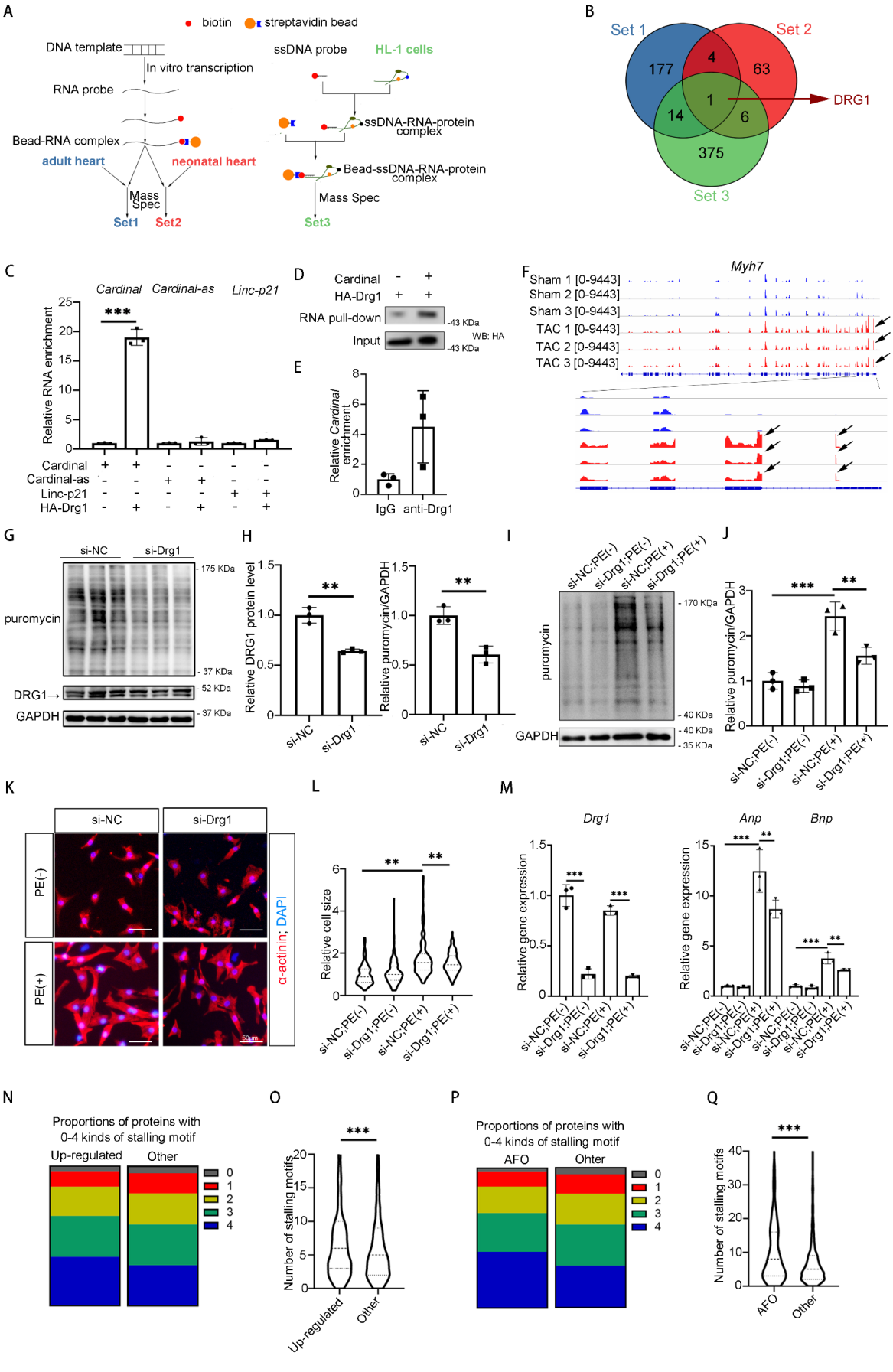
A
biotin
streptavidin bead
DNA template
In vitro transcription
RNA probe
Bead-RNA complex
adult heart
neonatal heart
Mass Spec
Set1
Set2
ssDNA probe
HL-1 cells
ssDNA-RNA-protein complex
Bead-ssDNA-RNA-protein complex
Mass Spec
Set3
B
Set 1
Set 2
Set 3
177
4
63
1
14
6
375
DRG1
C
Cardinal
Cardinal-as
Linc-p21
Relative RNA enrichment
***
Cardinal + + - - - -
Cardinal-as - - + + - -
Linc-p21 - - - - + +
HA-Drg1 - + - + - +
D
Cardinal - +
HA-Drg1 + +
RNA pull-down
-43 KDa
Input
WB: HA
-43 KDa
E
Relative Cardinal enrichment
IgG
anti-Drg1
F
Myh7
Sham 1 [0-9443]
Sham 2 [0-9443]
Sham 3 [0-9443]
TAC 1 [0-9443]
TAC 2 [0-9443]
TAC 3 [0-9443]
G
si-NC
si-Drg1
puromycin
175 KDa
37 KDa
DRG1
52 KDa
GAPDH
37 KDa
H
Relative DRG1 protein level
**
si-NC
si-Drg1
Relative puromycin/GAPDH
**
si-NC
si-Drg1
I
si-NC;PE(-)
si-Drg1;PE(-)
si-NC;PE(+)
si-Drg1;PE(+)
puromycin
170 KDa
40 KDa
GAPDH
40 KDa
35 KDa
J
Relative puromycin/GAPDH
***
**
si-NC;PE(-)
si-Drg1;PE(-)
si-NC;PE(+)
si-Drg1;PE(+)
K
si-NC
si-Drg1
PE(-)
PE(+)
α-actinin; DAPI
50μm
L
Relative cell size
**
**
si-NC;PE(-)
si-Drg1;PE(-)
si-NC;PE(+)
si-Drg1;PE(+)
M
Drg1
Anp
Bnp
Relative gene expression
***
***
***
***
***
**
si-NC;PE(-)
si-Drg1;PE(-)
si-NC;PE(+)
si-Drg1;PE(+)
N
Proportions of proteins with 0-4 kinds of stalling motif
Up-regulated
Other
0
1
2
3
4
O
***
Number of stalling motifs
Up-regulated
Other
P
Proportions of proteins with 0-4 kinds of stalling motif
AFO
Ohter
0
1
2
3
4
Q
***
Number of stalling motifs
AFO
Other

Figure 6. RNA interactome reveals that *CARDINAL* interacts with the translational regulator DRG1

A, Designs for 3 sets of RNA pull-downs. **B**, Venn plot showing the *Cardinal* interacting proteins. **C**, Relative enrichment of *Cardinal, Cardinal-as* and *Linc-p21* from HA-DRG1 and control immunoprecipitation. (N=3 for each group). **D**, Western blotting of HA-DRG1 in RNA pull-downs. **E,** Relative enrichment of *Cardinal* from immunoprecipitation in HL-1 cells. **F**, Ribo-seq coverages of hearts after sham or 2 weeks after TAC surgery (PRJNA484227) over the *Myh7* genomic locus (N=3 for each group). Black arrows showing a potential ribosome stalling site. **G,** Western blotting and **H,** quantification of DRG1 and puromycin incorporated protein in HL-1 cells 48 hours after RNA interference. Cells were treated by 1μM puromycin for 30 minutes before harvest. (N=3 for each group) **I,** Western blotting and **J,** quantification of puromycin incorporated protein in NRVCs 24 hours after stimulation.. Cells were treated by 1μM puromycin for 30 minutes before harvest (N=3 for each group). **K,** Immunofluorescent staining and **L,** cell size quantification of NRVCs 48 hours after stimulation (N≥300 for each group). **M**, RT-qPCR results of NRVCs 24 hours after stimulation (N=3 for each group). **I-M,** NRVCs were treated with si-NC or si-Drg1 and stimulated by culture medium with or without PE (50μM). **N**, Proportion of proteins with 0-4 categories of stalling motif among upregulated vs. the remaining proteins. **O**, Violin plots showing numbers of stalling motifs among upregulated vs. the remaining proteins. **P**, Proportion of proteins with 0-4 kinds of stalling motif among proteins in "Actin Filament Organization" (AFO) gene set vs. the remaining proteins. **Q**, Violin plots showing numbers of stalling motifs among proteins in AFO gene set vs. the remaining proteins. Statistical significance was tested by Student's T test (C and H), Mann-Whitney U test (O and Q), or ANOVA with Tukey's post hoc test (J, L, and M).

Figure 7

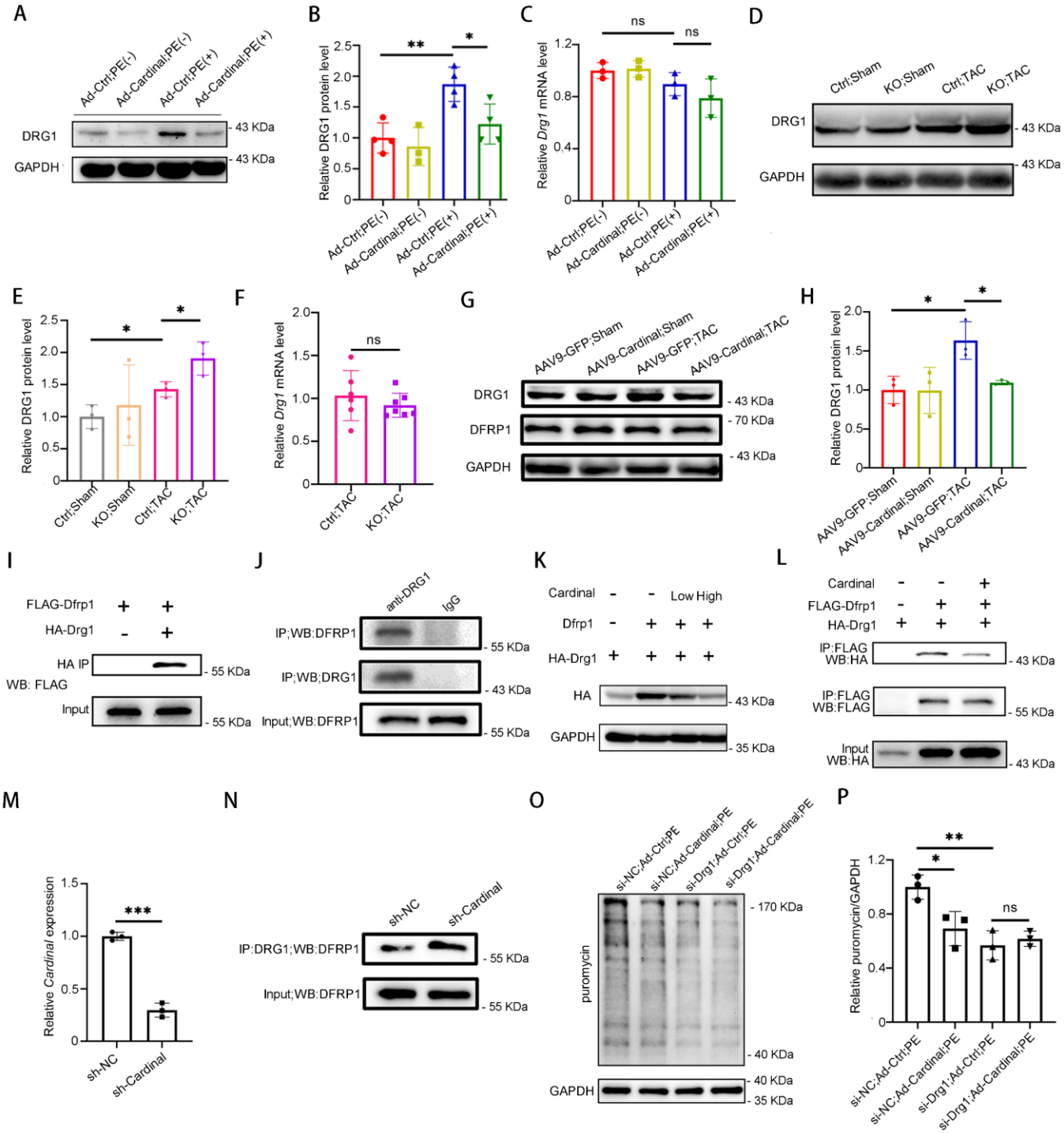
A
Ad-Ctrl;PE(-)
Ad-Cardinal;PE(-)
Ad-Ctrl;PE(+)
Ad-Cardinal;PE(+)
DRG1
GAPDH
43 KDa
43 KDa
B
Relative DRG1 protein level
**
*
Ad-Ctrl;PE(-)
Ad-Cardinal;PE(-)
Ad-Ctrl;PE(+)
Ad-Cardinal;PE(+)
C
Relative Drg1 mRNA level
ns
ns
Ad-Ctrl;PE(-)
Ad-Cardinal;PE(-)
Ad-Ctrl;PE(+)
Ad-Cardinal;PE(+)
D
Ctrl;Sham
KO;Sham
Ctrl;TAC
KO;TAC
DRG1
GAPDH
43 KDa
43 KDa
E
Relative DRG1 protein level
*
*
Ctrl;Sham
KO;Sham
Ctrl;TAC
KO;TAC
F
Relative Drg1 mRNA level
ns
Ctrl;TAC
KO;TAC
G
AAV9-GFP;Sham
AAV9-Cardinal;Sham
AAV9-GFP;TAC
AAV9-Cardinal;TAC
DRG1
DFRP1
GAPDH
43 KDa
70 KDa
43 KDa
H
Relative DRG1 protein level
*
*
AAV9-GFP;Sham
AAV9-Cardinal;Sham
AAV9-GFP;TAC
AAV9-Cardinal;TAC
I
FLAG-Dfrp1 + +
HA-Drg1 - +
HA IP
WB: FLAG
Input
55 KDa
55 KDa
J
anti-DRG1
IgG
IP;WB:DFRP1
IP;WB;DRG1
Input;WB:DFRP1
55 KDa
43 KDa
55 KDa
K
Cardinal - - Low High
Dfrp1 - + + +
HA-Drg1 + + + +
HA
GAPDH
43 KDa
35 KDa
L
Cardinal - - +
FLAG-Dfrp1 - + +
HA-Drg1 + + +
IP:FLAG WB:HA
IP:FLAG WB:FLAG
Input WB:HA
43 KDa
55 KDa
43 KDa
M
Relative Cardinal expression
***
sh-NC
sh-Cardinal
N
sh-NC
sh-Cardinal
IP:DRG1;WB:DFRP1
Input;WB:DFRP1
55 KDa
55 KDa
O
si-NC;Ad-Ctrl;PE
si-NC;Ad-Cardinal;PE
si-Drg1;Ad-Ctrl;PE
si-Drg1;Ad-Cardinal;PE
puromycin
170 KDa
40 KDa
GAPDH
40 KDa
35 KDa
P
Relative puromycin/GAPDH
**
*
ns
si-NC;Ad-Ctrl;PE
si-NC;Ad-Cardinal;PE
si-Drg1;Ad-Ctrl;PE
si-Drg1;Ad-Cardinal;PE

Figure 7. *CARDINAL* destabilizes DRG1 by preventing its interaction with DFRP1

A, Western blotting **B,** quantification of DRG1 protein level, and **C,** quantification of *Drg1* mRNA levels detected by RT-qPCR in NRVCs infected with control virus or Ad-*Cardinal* and treated with or without PE for 48 hours (50μM). (N⩾3 for each group) **D,** Western blotting and **E,** quantification of DRG1 protein level (N=3 for each group) and **F,** quantification of *Drg1* mRNA level (N⩾6 for each group) detected by RT-qPCR in hearts from control or *Cardinal*-KO mice 4 weeks after sham or TAC surgery. **G**, Western blotting analysis and **H,** quantification of DRG1 protein level in hearts from mice injected with AAV9-*GFP* or AAV9-*Cardinal* 4 weeks after sham or TAC surgery. (N=3 for each group) **I**, Western blotting of immunoprecipitated product and input in 293T cells showing interaction of DRG1 and DFRP1. **J,** Western blotting of anti-DRG1 or IgG immunoprecipitated product and input in HL-1 cells **K**, Western blotting of HA-DRG1 in 293T cells transfected by HA-Drg1 plasmid with or without co-transfection of *Dfrp1*and *Cardinal* plasmid. **L**, Western blotting of immunoprecipitated product and input of 293T cells showing effect of *Cardinal* on DRG1-DFRP1 interaction. The amount of transfected plasmid was carefully titrated to ensure comparable inputs in the presence or absence of *Cardinal*. **M**, Relative *Cardinal* level detected by RT-qPCR in sh-NC and sh-*Cardinal* HL-1 cells. (N=3 for each group). **N**, Western blotting of anti-DRG1 immunoprecipitated product in *Cardinal* stably knock-down (sh-*Cardinal*) and its control (sh-NC) HL-1 cells. **O,** Western blotting and **P,** quantification of puromycin incorporated protein in NRVCs with indicated treatment and PE stimulation for 9 hours (N=3 for each group). Statistical significance was tested by Student's T test (F and M) or ANOVA with Tukey's post hoc test (B, C, E, H, and P).

Figure 8

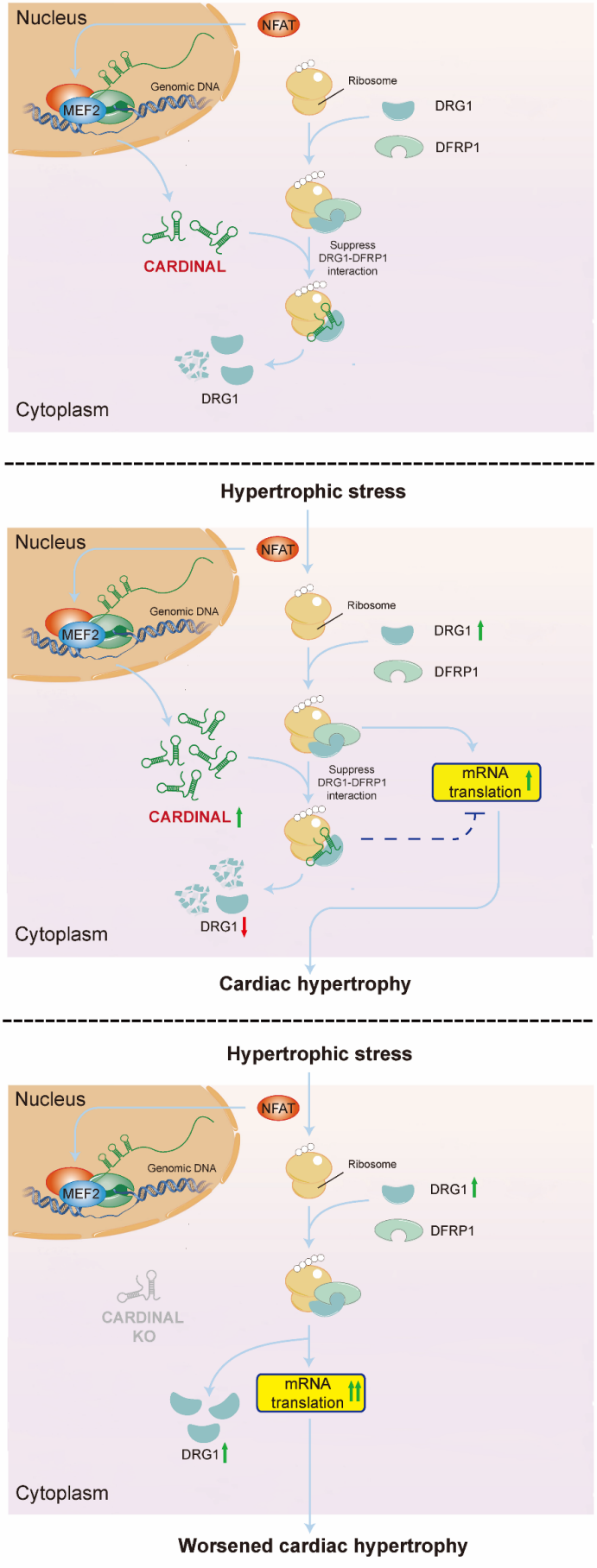
Nucleus
NFAT
Genomic DNA
MEF2
Ribosome
DRG1
DFRP1
CARDINAL
Suppress
DRG1-DFRP1
interaction
DRG1
Cytoplasm
Hypertrophic stress
Nucleus
NFAT
Genomic DNA
MEF2
Ribosome
DRG1
DFRP1
CARDINAL
Suppress
DRG1-DFRP1
interaction
mRNA
translation
DRG1
Cytoplasm
Cardiac hypertrophy
Hypertrophic stress
Nucleus
NFAT
Genomic DNA
MEF2
Ribosome
DRG1
DFRP1
CARDINAL
KO
mRNA
translation
DRG1
Cytoplasm
Worsened cardiac hypertrophy

Figure 8. A proposed model for the regulation of mRNA translation and cardiac hypertrophy by *CARDINAL*

Panel 1, *Cardinal* is a cardiac-specific lncRNA that can suppress mRNA translation. Under normal conditions, the expression of *Cardinal* and the ribosome binding protein DRG1 (which promotes mRNA translation) are in balance. We propose that *CARDINAL* inhibits mRNA translation by interference with DRG1 function. *CARDINAL* binds DRG1 and interferes with the formation of the DRG1-DFRP1 stabilization complex; inhibition of DRG1-DFRP1 complex formation by *CARDINAL* results in reduced levels of DRG1 which helps maintain a normal level of translation. **Panel 2**, Under stress conditions, both the lncRNA *CARDINAL* and DRG1 are upregulated. However, while *Cardinal* attempts to inhibit cardiomyocyte translation it is no longer able to balance the increased translation induced by the increase in DRG1; the result is a net increase in mRNA translation and cardiac hypertrophy. **Panel 3**, In the absence of *Cardinal*, the constraint on DRG1 levels is lost. The result is an even greater elevation in protein synthesis and worsening of cardiac hypertrophy.